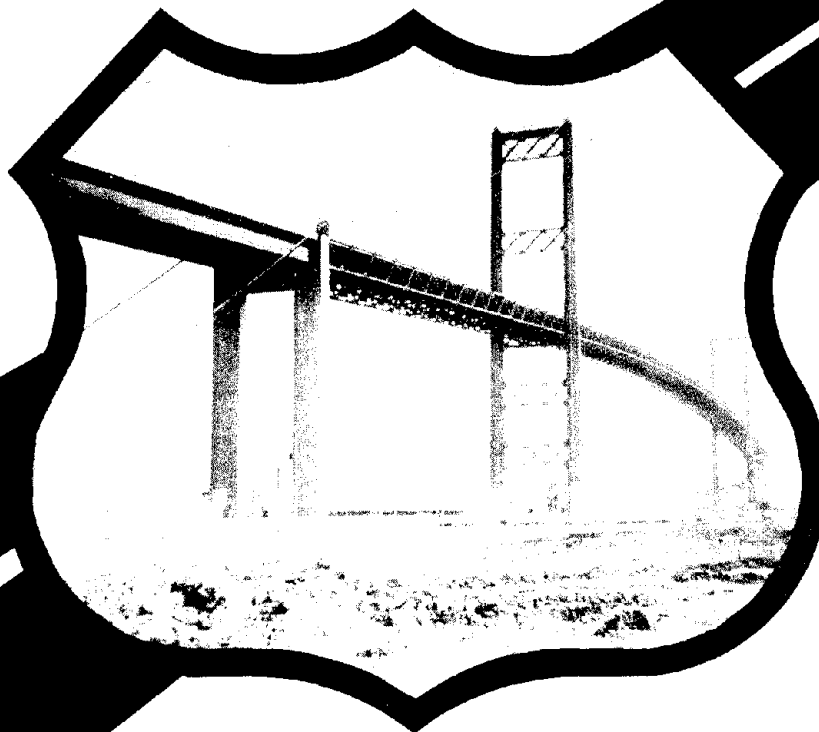


Report No. FHWA/RD-80/050

STATE-OF-THE-ART METHODS FOR CALCULATING FLUTTER, VORTEX-INDUCED, AND BUFFETING RESPONSE OF BRIDGE STRUCTURES

April 1981
Final Report



Document is available to the public through
the National Technical Information Service,
Springfield, Virginia 22161



Prepared for
FEDERAL HIGHWAY ADMINISTRATION
Offices of Research & Development
Structures and Applied Mechanics Division
Washington, D.C. 20590

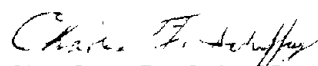
REPRODUCED BY
**NATIONAL TECHNICAL
INFORMATION SERVICE**
U.S. DEPARTMENT OF COMMERCE
SPRINGFIELD, VA. 22161

FOREWORD

This report presents recent methods for predicting wind-induced responses of long-span bridge structures using results obtained from wind tunnel tests on models. The report will be of interest to bridge engineers and researchers involved in the analysis, design, research, and construction of large bridge structures.

The research documented in this report was done as part of the Federal Highway Administration FCP Program. Results are being integrated into FCP Project 5 A entitled "Improved Protection Against Natural Hazards of Earthquake and Wind." Mr. James D. Cooper is the project manager and Mr. Harold R. Bosch is the task manager.

Sufficient copies of the report are being distributed to provide a minimum of one copy to each regional office, one copy to each division office, and two copies to each State highway department. Direct distribution is being made to the division offices.



Charles F. Scheffey
Director, Office of Research
Federal Highway Administration

NOTICE

This document is disseminated under the sponsorship of the Department of Transportation in the interest of information exchange. The United States Government assumes no liability for its contents or use thereof. The contents of this report reflect the views of the contractor, who is responsible for the accuracy of the data presented herein. The contents do not necessarily reflect the official views or policy of the Department of Transportation. This report does not constitute a standard, specification, or regulation.

The United States Government does not endorse products or manufacturers. Trade or manufacturers' names appear herein only because they are considered essential to the object of this document.

1. Report No. FHWA/RD - 80/050		2. Government Accession No.		3. Recipient's Catalog No. FD-302 25697.5	
4. Title and Subtitle State-of-the-Art Methods for Calculating Flutter, Vortex-Induced, and Buffeting Response of Bridge Structures				5. Report Date April 1981	
				6. Performing Organization Code	
7. Author(s) Robert H. Scanlan				8. Performing Organization Report No.	
9. Performing Organization Name and Address Robert H. Scanlan 34 Burning Tree Lane Lawrenceville, New Jersey 08648				10. Work Unit No. (TRAIS) FCP 35A1 - 102	
				11. Contract or Grant No. P.O.# 9-3-0107	
12. Sponsoring Agency Name and Address Federal Highway Administration Office of Research 400 7th St. SW Washington, D.C. 20590				13. Type of Report and Period Covered Final Report	
				14. Sponsoring Agency Code 801235	
15. Supplementary Notes FHWA Contract Manager: H.R. Bosch (HRS-11)					
16. Abstract A unified body of theory is presented to cover the main phenomena of the wind-induced responses of long-span bridges. The methods discussed depend strongly upon experimental data extracted through aeroelastic tests of bridge deck section models. Much of the background material stems from Report No. FHWA-RD-75-115 : "Recent Methods in the Application of Test Results to the Wind Design of Long, Suspended-Span Bridges", Federal Highway Administration, Offices of Research and Development, Washington, D.C. (October 1975). The sections of the present report are: I. Introduction and Overview II. The Background Literature III. Analytics of the Flutter Problem IV. A Vortex-Shedding Model in the Bridge Context V. Parameters Affecting Long-Span Bridge Buffeting Susceptibility VI. Conclusions The Report contains calculated examples of all phenomena discussed.					
17. Key Words Wind response, long-span, bridges, aerodynamics, aeroelasticity, flutter, vortex-shedding, model, buffeting, test, turbulence, design.			18. Distribution Statement No restrictions. This document is available to the public through the National Technical Information Service, Springfield, Virginia 22161.		
19. Security Classif. (of this report) Unclassified		20. Security Classif. (of this page) Unclassified		21. No. of Pages 116	22. Price

TABLE OF CONTENTS

	<u>Page</u>
I. INTRODUCTION AND OVERVIEW	1
II. THE BACKGROUND LITERATURE	4
2.1 Basic Modeling Technique	4
2.2 The Extraction of Aerodynamic Data from Models	9
2.3 Literature on the Flutter Problem	10
2.4 Literature on the Buffeting Problem	12
2.5 Literature on the Vortex-Shedding Problem	14
References for Section II	15
III. ANALYTICS OF THE FLUTTER PROBLEM	22
3.1 The 2-D Problem	22
3.2 The 3-D Problem	28
3.3 Case of an Arched or Curved Deck	30
3.4 Solutions of the Flutter Equations	34
3.4.1 Simplest Case: Pure Torsional Flutter	34
3.4.2 The Two-Degree-of-Freedom Case for Straight Decks	36
Example of Pure Torsional Flutter	38
Example of Two-Degree Flutter	39
References for Section III	48
IV. A VORTEX SHEDDING MODEL IN THE BRIDGE CONTEXT	49
Introduction	49
4.1 Analytical Model of the Deck Section	55
4.2 Evaluation of Constants in the Analytical Model	56
4.3 Analytical Model of the Full Bridge	58
4.4 Example	61
4.5 Correction for Loss of Spanwise Coherence	62
4.6 Remarks on Torsional Response	67
References for Section IV	70

	<u>Page</u>
V. PARAMETERS AFFECTING LONG-SPAN BRIDGE BUFFETING SUSCEPTIBILITY	71
Introduction	71
5.1 Theory for Torsion	72
5.2 Discussion of Factors Affecting the Variance in Torsion	80
5.3 Examples in Torsion	84
5.4 Discussion and Conclusions Relative to Torsion	89
5.5 Theory for Bending	91
5.6 Discussion of Factors Affecting the Variance in Bending	95
5.7 Examples in Bending	97
References for Section V	100
VI. CONCLUSIONS	101

LIST OF TABLES

TABLE		<u>page</u>
4.1	Strouhal Number for Typical Structural Sections	52
5.1	Surface Roughness Length	78
5.2	Buffeting Data for $\bar{U} = 13.4$ meters/sec	85
5.3	Buffeting Data for $\bar{U} = 26.8$ meters/sec	86
5.4	Buffeting Data for $\bar{U} = 40.2$ meters/sec	86
5.5	Summary of Torsional Buffeting Results	87
5.6	Maximum Expected Excursions - Torsional Buffeting	87
5.7	Maximum Buffeting Displacements - Torsion	90
5.8	$\bar{U}^{2.833}$ Law versus Results of Melbourne	90
5.9	Bending Mode Data	98
5.10	Buffeting Data for $\bar{U} = 13.4$ meters/sec	98
5.11	Buffeting Data for $\bar{U} = 26.8$ meters/sec	99
5.12	Buffeting Data for $\bar{U} = 40.2$ meters/sec	99

LIST OF FIGURES

FIGURE		<u>page</u>
2.1	Section Model in G.S. Vincent Wind Tunnel	8
3.1	Degrees of Freedom for Deck Section	23
3.2	Aerodynamic Coefficients	26
3.3	Aerodynamic Coefficients	27
4.1	Frequency Characteristics of Vortex Shedding	53
4.2	Correlation of Vortex Shedding from Circular Cylinder at Lock-in	63

METRIC CONVERSION FACTORS

APPROXIMATE CONVERSIONS FROM METRIC MEASURES

SYMBOL WHEN YOU KNOW MULTIPLY BY TO FIND SYMBOL

LENGTH

in	inches	2.5	centimeters	cm
ft	feet	30	centimeters	cm
yd	yards	0.9	meters	m
mi	miles	1.6	kilometers	km

AREA

in ²	square inches	6.5	square centimeters	cm ²
ft ²	square feet	0.09	square meters	m ²
yd ²	square yards	0.6	square meters	m ²
mi ²	square miles	2.6	square kilometers	km ²
	acres	0.4	hectares	ha

MASS (weight)

oz	ounces	28	grams	g
lb	pounds	0.45	kilograms	kg
	short tons (2000 lb)	0.9	tonnes	t

VOLUME

tsp	teaspoons	5	milliliters	ml
tbsp	tablespoons	15	milliliters	ml
fl oz	fluid ounces	30	milliliters	ml
c	cups	0.24	liters	l
pt	pints	0.47	liters	l
qt	quarts	0.95	liters	l
gal	gallons	3.8	liters	l
ft ³	cubic feet	0.03	cubic meters	m ³
yd ³	cubic yards	0.76	cubic meters	m ³

TEMPERATURE (exact)

°F	Fahrenheit temperature	5/9 (after subtracting 32)	Celsius temperature	°C
----	------------------------	----------------------------	---------------------	----

APPROXIMATE CONVERSIONS FROM METRIC MEASURES

SYMBOL WHEN YOU KNOW MULTIPLY BY TO FIND SYMBOL

LENGTH

mm	millimeters	0.04	inches	in
cm	centimeters	0.4	inches	in
m	meters	3.3	feet	ft
m	meters	1.1	yards	yd
km	kilometers	0.6	miles	mi

AREA

cm ²	square centimeters	0.16	square inches	in ²
m ²	square meters	1.2	square yards	yd ²
km ²	square kilometers	0.4	square miles	mi ²
ha	hectares (10,000m ²)	2.5	acres	

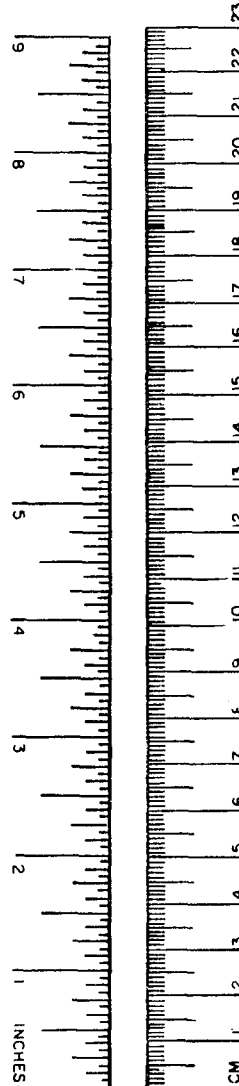
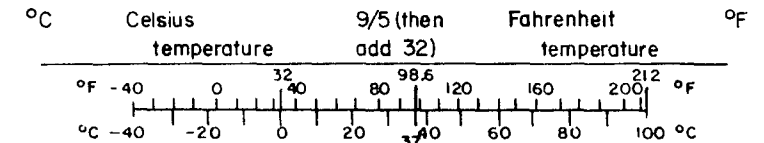
MASS (weight)

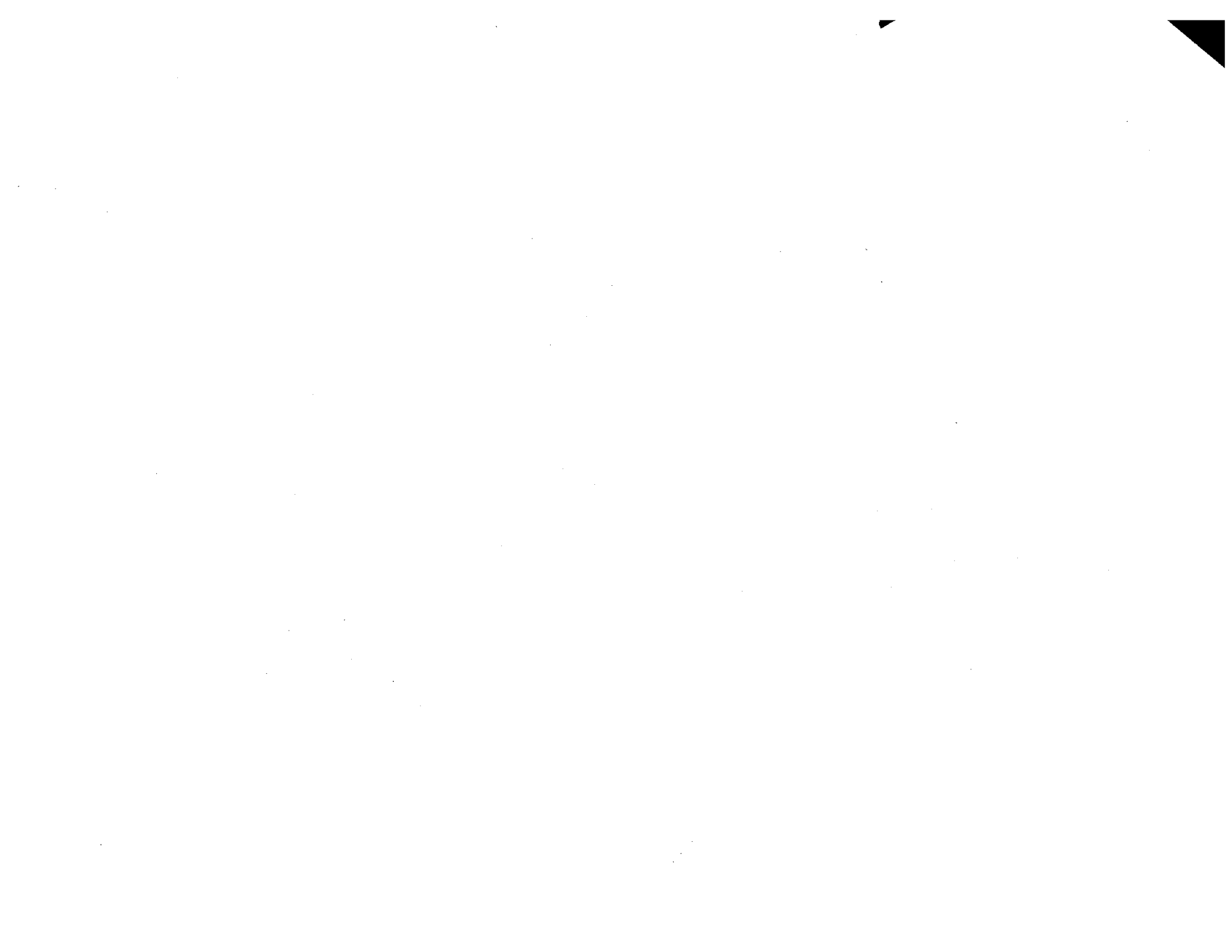
g	grams	0.035	ounces	oz
kg	kilograms	2.2	pounds	lb
t	tonnes (1000kg)	1.1	short tons	

VOLUME

ml	milliliters	8.03	fluid ounces	fl oz
l	liters	2.1	pints	pt
l	liters	1.06	quarts	qt
l	liters	0.26	gallons	gal
m ³	cubic meters	36	cubic feet	ft ³
m ³	cubic meters	1.3	cubic yards	yd ³

TEMPERATURE (exact)





STATE-OF-THE-ART METHODS FOR CALCULATING FLUTTER, VORTEX-INDUCED, AND BUFFETING RESPONSE OF BRIDGE STRUCTURES

I. INTRODUCTION AND OVERVIEW

It is matter of historical record that, prior to the pivotal Tacoma Narrows incident, many suspended-span bridges were destroyed by wind. It was only with Tacoma Narrows, however, that a deep general realization of the potential aeroelastic nature of these phenomena was firmly inaugurated. This general insight was based primarily on the results of tests of bridge section models in wind tunnels. Although by the present date perhaps a dozen or more full-bridge aeroelastic models have been built and tested, the test method of choice for the far larger number remains the section model, even including those cases where other model types are also studied.

The prime advantages of the section model are its relative cheapness and simplicity, coupled with the fact that it can be made large enough to give rather faithful attention to geometric detail to avoid some of the questionable Reynolds number problems of smaller-scale models.

The original focus of aeroelastic studies on bridge models was the flutter problem, since flutter had destroyed the original Tacoma Narrows span. Flutter is a self-excited oscillation that sets in at some critical cross-wind velocity and does not diminish, but instead increases in severity, at higher velocities. Self-excitation is its key characteristic, whereby bridge structural oscillatory deflection induces wind forces that enhance such motion.

The severity of the example set out at Tacoma Narrows was sufficient that today it would be considered a huge oversight in flexible, long-span bridge design if wind tunnel aeroelastic studies were not routinely prescribed. By the same token, the problem of bridge flutter may be considered to be under design control in the present state of the art. This does not imply that the problem is routinely dispensed with, but rather that the means are at hand, and quite fully understood, to alleviate it, most particularly if they are applied in the design stage rather than as a post-construction "fix".

This report will first address itself to the flutter problem, outlining the steps necessary to treat it through the study of wind tunnel section models plus analysis.

There remain two wind-induced problems of long-span flexible bridges which may be generally classed rather as annoying than as potentially catastrophic. These are the responses to vortex induction around the deck and to buffeting by wind turbulence. Each of those will be treated in this report also.

Vortices are shed behind any bluff body in a cross flow. The general regularity of such shedding, accompanied by alternating pressures over the body, may excite one of the natural frequencies of the body. This occurs over many bridge decks, particularly those having bluff, solid cross-sections. An oscillation may be set up that, while not proceeding at higher wind velocities to catastrophic proportions, may still be very objectionable from a user or a fatigue standpoint. The suppression of vortex-induced oscillations at relatively low wind speeds may in fact be a slightly more troublesome problem to alleviate than the more fundamental and dangerous problems of

flutter. Even bridges that are not flutter-prone may occasionally exhibit a susceptibility to vortex-induced excitation. Again, adequate aerodynamic treatment in the design stage can be counted on for alleviation. This report concerns itself with analytical models which may assist in extrapolating model data on vortex response to full scale, for use in predicting prototype action.

Finally, a problem to which all bridge designs remain more or less susceptible, regardless of their other aerodynamic treatments, is that of buffeting. The wind, being turbulent, attacks the bridge deck from a range of angles about the horizontal. In other words, the natural wind contains velocity vectors that are not all simultaneously oriented in the mean horizontal direction. These impinge on the bridge and give rise to varying transient pressure distributions that are random in space and in time. Depending on the spectral distributions of these velocity vectors, they may selectively excite certain modes of vibration in the full bridge. The design problem is to ascertain whether such possible excitation will be harmful to the bridge over its lifetime, from either a user comfort or fatigue standpoint, and to influence those design parameters that counteract buffeting effects.

Based on certain data taken on the deck section model, reliable calculations of expected buffeting response can be made. Such calculations aid in establishing important design information such as expected stress levels, desirable torsional stiffness values, etc. This report offers techniques for making such analytical estimates.

II. THE BACKGROUND LITERATURE

Serious analytical and experimental studies relative to the problems of bridge aeroelasticity began, of course, in 1940, with Tacoma Narrows. The monumental work of Farquharson [2.1]* containing key sections by Karman and Dunn (Part III, Ch. VII) went a very long way, not only in diagnosing the faults of the original Tacoma design and developing a stable configuration for its replacement, but in launching modern practice relative to such problems.

Excellent early work on bridge deck section models was done by Scruton [2.4] and others at the National Physical Laboratories (now National Maritime Institute) Teddington, England (see Refs. [2.12], [2.29], [2.63] for a rather extensive bibliography). In the same spirit, George Vincent pursued section model aerodynamic studies in the 1950's in the wind tunnel which he designed and had built (and which now bears his name) at the Fairbank Highway Research Station of the U.S. Federal Highway Administration at McLean, Virginia.

A good deal of testing of section models took place in the 1950's and early 1960's, most of which centered on a conception of the model as a direct analog of the prototype bridge. A representative set of references covering this period may be found in [2.12].

2.1 Basic Modeling Technique

In order to explain the trends in the extensive literature, it is worthwhile at this point to discuss the modern viewpoints on model testing.

Flutter, as an aeroelastic phenomenon, depends strongly upon:

1. aerodynamics, as influenced decisively by the geometry of the bridge structure;
2. bridge structural dynamics, resulting motions of which interact ("aeroelastically") with bridge aerodynamics.

* Numbers in brackets refer to the listing at the end of Section II.

Thus, the prime objective of bridge model dynamic tests is to establish a geometric configuration that will be stable against flutter in the wind.

Therefore, the first use of models is to establish this configuration. For this, the model must *approximate* a dynamically scaled version of the bridge. (It cannot, however, be hoped that more than a first approximation in this sense can be achieved since, ultimately, the dynamic characteristics of a section model fall far short of those of a full bridge.) A desirable level of approximation is achieved, however, first, by establishing simple scales for testing under laminar wind flow, as follows:

- 1) length scale (λ_L), model (m)-to-prototype (p):

$$\lambda_L = L_m/L_p$$

- 2) wind velocity scale (λ_U):

$$\lambda_U = U_m/U_p$$

usually set by available tunnel wind speeds compared to natural high wind speeds at the site of the prototype.

- 3) Density Scale (λ_ρ):

$$\lambda_\rho = \frac{\rho_m}{\rho_p} = 1$$

This must be unity since both the model and the prototype are immersed in air of the same density (on the occasion of model testing at altitude or in gas of another density $\lambda_\rho \neq 1$ and must be adjusted accordingly.)

- 4) Equal reduced velocity condition (maintenance of flow geometric similarity under oscillatory motion)

$$\left(\frac{U}{NB}\right)_m = \left(\frac{U}{NB}\right)_p$$

(N and B are structural natural frequency and typical dimension, like bridge deck width, respectively). This results in the frequency scaling law:

$$\lambda_N = \lambda_U / \lambda_L$$

Note that if equal gravitational effects (as might occur with pendulum action of a suspended span) are required, then Froude scaling may apply, according to which:

$$\left(\frac{U^2}{Bg}\right)_m = \left(\frac{U^2}{Bg}\right)_p$$

Since $g = g_m = g_p$ (model and prototype are under the same gravitational acceleration g), then

$$\lambda_U^2 / \lambda_L = 1$$

or

$$\lambda_U = \sqrt{\lambda_L}$$

and therefore frequency scaling follows the law:

$$\lambda_N = 1 / \sqrt{\lambda_L}$$

under Froude scaling.

Inversely, time scaling follows as

$$\lambda_T = 1 / \lambda_N = \sqrt{\lambda_L}$$

under Froude scaling; or

$$\lambda_T = \lambda_L/\lambda_U$$

under general scaling.

- 5) Finally, oscillation damping (in terms of log dec δ and critical damping ratio ζ ; $\delta \approx 2\pi\zeta$) must satisfy

$$\zeta_m/\zeta_p = \lambda_\zeta = 1$$

The model consists typically of a rigid, carefully constructed, geometric scale-replica of a chosen abbreviated length of the bridge suspended span (see, for example, Fig. 2.1). This model is then endowed with bending (vertical) and torsional (rotational) freedoms by mounting it elastically upon springs. The springs are usually outside the air flow. The calibration and spacing of the springs is such that, following the modeling laws, the lowest bending and torsional frequencies of the full bridge are reproduced to scale in the section model.

Model damping should duplicate prototype damping, which is initially unknown. It is then usually conservative to take model damping as low as reasonably possible.

In this first configuration, then, the model is *provisionally* assumed to represent the action of a typical section of the prototype, principally for purposes of working on its aerodynamic shape. Several alternate geometric configurations are typically prepared and wind-tunnel tested for direct observation of the model's aerodynamic stability over a range of wind velocities. That which is most stable or stable over the widest range is tentatively elected as the prototype configuration.

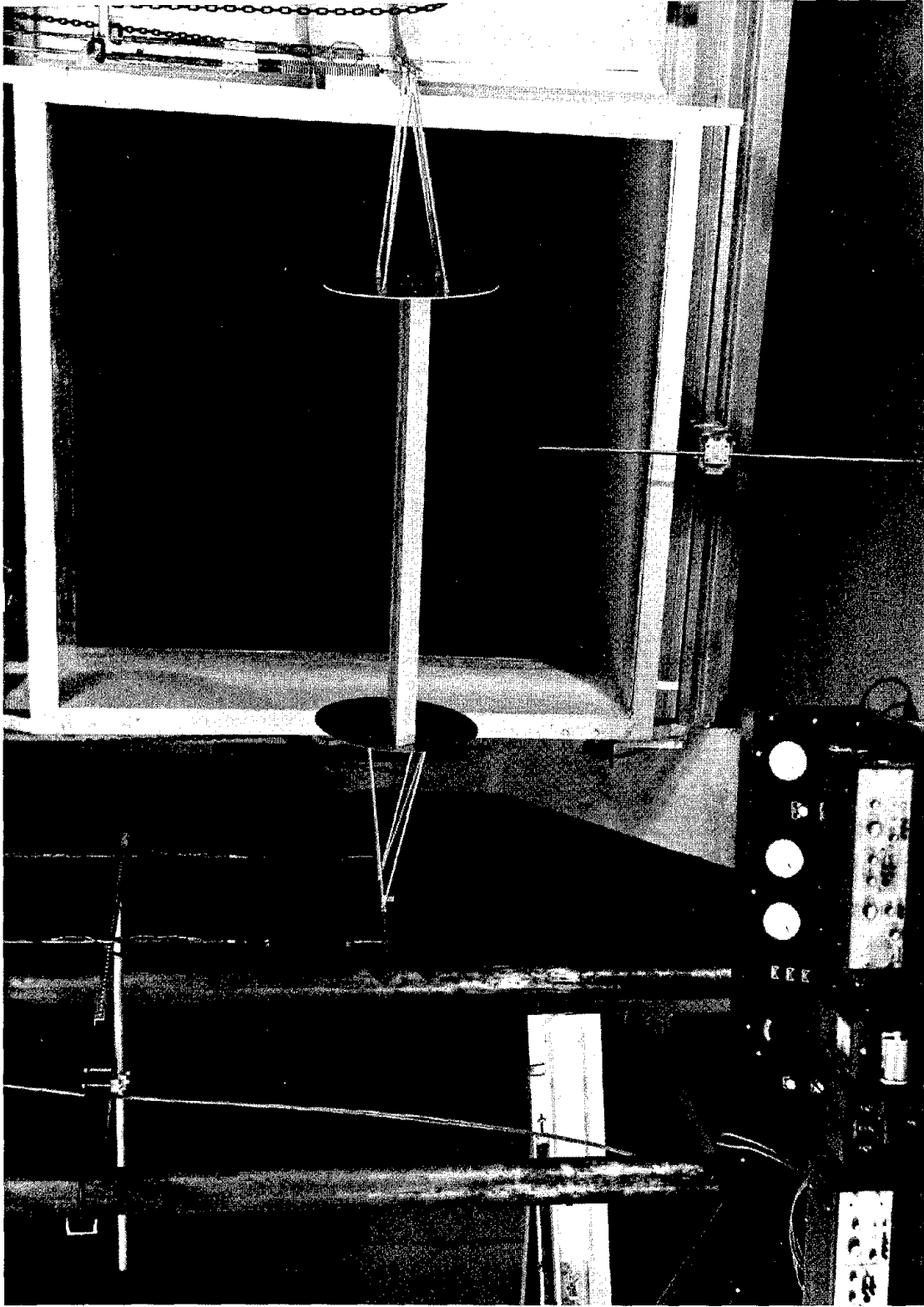


FIGURE 2.1: SECTION MODEL IN G.S. VINCENT WIND TUNNEL

2.2 The Extraction of Aerodynamic Data from Models

The more modern viewpoint on models in the wind tunnel is that they are in reality analog computers capable of yielding basic aerodynamic force information. Such information is useful in making a variety of predictive and diagnostic calculations for study of the prototype bridge responses to wind.

Starting in the mid-1960's (see Refs. [2.11], [2.14]), this more analytic use of models began to be exploited. Refs. [2.16] and [2.29] describe in detail how models may be studied to extract information on their so-called *flutter derivatives*.

Without making explicit use here of analysis at this point, the experimental data that models can furnish for ultimate analysis purposes, can be described:

1. Static: Aerodynamic lift, drag, and moment coefficients.
2. Dynamic: Flutter derivatives for the oscillating bridge deck.
3. Dynamic: Indicial lift and moment functions for the bridge deck.
4. Aerodynamic admittance of the bridge deck in turbulent flow.

The concerns of much of the literature in the recent two decades have centered on *analytic* studies of bridge response, with a necessary minimum of basic input data expected to stem from section model studies. Certain papers emphasize the techniques of extraction of the data from models, while other papers emphasize the development of theories for bridge response in which model experimental data play central roles.

2.3 Literature on the Flutter Problem

This literature is the oldest and most voluminous. Good summaries are available in Refs. [2.12], [2.29] and [2.63]. It is not worthwhile to emphasize, at this late date, the long list of studies in which the section model is viewed and employed primarily in the "first" way, i.e. as an approximate direct analog of the prototype. Such studies have become classic as well as indispensable and are made in a straightforward manner in perhaps a dozen laboratories around the world. One might comment that the "modern" literature begins approximately where these studies cease, i.e. it starts with a concern for the section models as analog computers of aerodynamic forces and admittances rather than as analog computers of the entire gamut of possible prototype bridge responses under wind.

The modern era of interpretation of section models can perhaps be said to have been inaugurated approximately in the mid-1960's. At a conference on suspension bridges held in 1966 in Lisbon, at the inauguration of the new Tagus River bridge, a paper by Ukeguchi, Sakata, and Nishitani [2.11] appeared that revealed the basic method developed in Japan for experimentally measuring the flutter derivatives (aerodynamic coefficients accompanying bridge deck oscillation) of bridge decks and for using these results in analytical bridge flutter stability studies.

This paper described the method, now widely accepted in Japan, of using a machine to drive a rigid bridge deck section model through certain prescribed oscillation amplitudes, at a range of frequencies in the wind tunnel. A description was given of the method of obtaining the aerodynamic forces engendered on the model while it was thus oscillated; a key item was the simultaneous oscillation of a "dummy" model outside the air stream, in

order to develop equal and opposite inertial forces which were then subtracted from the measured total force to obtain the net forces of aerodynamic origin. This very effective method generally follows out the techniques of a very similar method initiated in the 1950's at MIT by Halfman [2.2] who measured airfoil flutter derivatives by it.

Late in 1967, the so-called "free-oscillation" technique was initiated in the United States at the George Vincent Wind Tunnel of the FHWA by Scanlan and Sabzevari and later more fully exploited by Scanlan and Tomko. This method is fully described in Refs. [2.14], [2.16] and [2.29]. Essentially, the method allows the free oscillation of the bridge deck model in a cross wind and infers the appropriate flutter derivatives from identification techniques applied to the study of the model oscillatory response at various values of the reduced velocity parameter U/NB . The main advantage of the technique is its relative simplicity and its lack of requirements for extensive experimental hardware.

A third technique for obtaining bridge model flutter derivatives was developed in France by Loiseau and Széchenyi [2.25], who drove a bridge model through prescribed oscillation amplitudes and measured the oscillatory pressure changes at a series of taps on the surface of the model. The varying pressures were then integrated spacewise to obtain net motion-dependent aerodynamic forces on the model. This very effective method requires a reasonable provision of calibrated, highly sensitive pressure measuring and recording equipment. Its use is limited, in certain circumstances, by the presence of special geometric forms in the bridge deck section, such as fences, parapets, or barriers, in which pressure taps may not be conveniently located for testing purposes.

All three of the above methods provide flutter derivatives which cannot, to date, be obtained other than by experiment, given the aerodynamic complexity of typical bridge deck cross-sections. It remains necessary, after such experiments, to continue dynamic analysis of bridge performance based on their results. Refs. [2.12], [2.29], and [2.54] detail the manner in which bridge deck flutter analyses may be carried out. The present report also highlights key aspects of these methodologies.

The principal advantage of the modern analytic interpretation of bridge section model experiments is that, after a minimum of aerodynamic experimentation, the flutter problem is transferred over to a calculational form that permits a wide variation of parameters, including full-prototype simulation under a variety of assumed conditions not necessarily present in the laboratory. Also, since the experimentally derived data reflect only the geometric effects of the bridge deck shape, and not its inertial or elastic dynamics, the section model tests themselves can be made under simplified conditions not necessarily reflecting complete prototype conditions. The model is then construed merely as a geometric representative of the prototype, not as complete in all dynamic details. Thus prototype damping, frequencies, etc, need not be accurately scaled in the test (although it is sound practice not to depart too strongly from expected ranges for them). The data obtained are dimensionless functions of reduced cross-wind velocity U/NB and as such are directly transferable to the prototype.

2.4 Literature on the Buffeting Problem

The problems of flutter and buffeting of suspended-span bridges bear certain generic resemblances to the aircraft problems of the same names.

Though bridge problems are distinguished by flows around generally bluff bodies, while aircraft problems center on streamlined ones, the broad outlines of the analytic approaches to both categories of problem are very similar. The specific points on which they differ will be emphasized later.

In 1952, Liepmann [2.3] published a paper on the response of aircraft to atmospheric gusts. In 1961 and 1962, Davenport [2.6], [2.7] and [2.8] published what are probably the first analytic papers to appear on the effect of wind turbulence on slender structures and suspension bridges. In 1966, he presented another, more extended paper [2.10], on the same subject at the Lisbon suspension bridge conference. In 1971, Simiu, in a doctoral dissertation [2.17] at Princeton University, described methods for calculating the response of a bridge to buffeting.

In 1975, Holmes [2.22], presented a theoretical calculation of the response of a cable-stayed bridge to turbulent wind.

In 1977, Scanlan and Gade [2.43] offered a method that included experimentally measured, aerodynamic ("flutter") derivatives.

In 1978, Scanlan presented two comprehensive papers [2.55] on the experimentally-derived section model flutter and static force derivatives. This work suggested analytical arguments for the observed fact that flutter of a full bridge in turbulent wind does not necessarily exhibit a sharp critical onset at a specific velocity (as does a flutter model in laminar flow). This was explained by the effect of the aerodynamic coupling, through the flutter derivatives, in distributing the wind energy throughout several bridge modes simultaneously, instead of permitting a concentration of energy in just the lowest unstable mode.

Further contributions to analytical bridge buffeting predictions were made in 1978 by Irwin and Schuyler [2.51], [2.52], who dealt with both experimental and analytic predictions of the wind response of the Lions' Gate bridge.

Holmes [2.49] has developed an analytical prediction of the response of the West Gate bridge to turbulent wind.

Studies in Japan, notably [2.23 - 2.24], [2.26-2.28], [2.33-2.35] and [2.45], have dealt with the prediction of buffeting response.

The present report will select and present a single basic approach to the analytical buffeting problem in a later section.

2.5 Literature on the Vortex-Shedding Problem

The general vortex-shedding problem for bluff bodies has a very extensive literature, some of which is cited in [2.54](Chs. 4,6,8). A very good general compilation on the vortex-shedding problem for individual bridge structural members, has been made by Chi et al [2.30], [2.36], for the U.S. Federal Highway Administration. For applications specifically to bridge decks, few references, aside from [2.54] (Ch. 6) and [2.29], may be cited.

The present report will offer, at a later point, an analytical methodology based on deck section model experiments. Not all the references compiled and listed in this report are specifically cited, only the principal highlights being mentioned in the above review. The longer reference list is retained at the end of this section, however, for its broad value to the interested reader.

REFERENCES FOR SECTION II

1949

- [2.1] Farquharson, F.B., ed.: Aerodynamic Stability of Suspension Bridges, Univ. of Washington Engrg. Exper. Sta. Bulletin, No. 116, Parts I-V, June 1949 - June 1954.

1952

- [2.2] Halfman, R.L.: "Experimental Aerodynamic Derivatives of a Sinusoidally Oscillating Airfoil in Two-Dimensional Flow," NACA Report 1108, National Aeronautics and Space Administration (formerly NACA), 1952.
- [2.3] Liepmann, H.W.: "On the Application of Statistical Concepts to the Buffeting Problem," Jnl. Aeron. Sci. Vol. 19, No. 12, Dec. 1952, pp. 798 - 800, 822.
- [2.4] Scruton, C.: "Experimental Investigation of Aerodynamic Stability of Suspension Bridges with Special Reference to Proposed Severn Bridge," Proc. Inst. of Civil Engrs., London, Vol. 1, Part 1, No. 2, March 1952, pp. 189-222.

1958

- [2.5] Keulegan, G.H. and Carpenter, L.H.: "Forces on Cylinders and Plates in an Oscillating Fluid," Jnl. Res. Nat'l. Bur. Std., Vol. 60, No. 5, May 1958, pp. 423-440.

1961

- [2.6] Davenport, A.G.: "The Application of Statistical Concepts to the Wind Loading of Structures," Proc. Inst. Civ. Engrs., London, U.K., Vol. 19, 1961, pp. 449-472.

1962

- [2.7] Davenport, A.G.: "The Response of Slender, Line-Like Structures to a Gusty Wind," Proc. Inst. Civ. Engrs., London, U.K., Vol. 23, 1962, pp. 389-407.
- [2.8] Davenport, A.G.: "Buffeting of a Suspension Bridge by Storm Winds," Jnl. Struc. Div., Proc. Amer. Soc. Civ. Engrs., June, 1962, pp. 233-264.

1964

- [2.9] Davenport, A.G.: "Note on the Distribution of the Largest Value of a Random Function with Application to Gust Loading," Proc. Inst. Civ. Eng., London, U.K., Vol. 28, 1964, pp. 187-196.

1966

- [2.10] Davenport, A.G.: "The Action of Wind on Suspension Bridges," Proc. Int'l. Sympos. on Suspension Bridges, Laboratorio Nacional de Engenharia Civil, Lisbon, Portugal, 1966, pp. 79-100.
- [2.11] Ukeguchi, N., Sakata, H. and Nishitani, H.: "An Investigation of Aeroelastic Instability of Suspension Bridges," Proc. Int'l. Sympos. on Suspension Bridges, Laboratorio Nacional de Engenharia Civil, Lisbon, 1966, pp. 79-100.

1968

- [2.12] Sabzevari, A. and Scanlan, R.H.: "Aerodynamic Instability of Suspension Bridges," Jn. Eng. Mech. Div., Proc. Amer. Soc. Civ. Eng., Vol. 94, April 1968, pp. 489-519.

1969

- [2.13] Davenport, A.G., et al.: "A Study of Wind Action on a Suspension Bridge During Erection and on Completion," BLWT-3-69, Boundary Layer Wind Tunnel Laboratory, Univ. of Western Ontario, London, Canada, May 1969.
- [2.14] Scanlan, R.H. and Sabzevari, A.: "Experimental Aerodynamic Coefficients in the Analytical Study of Bridge Flutter," Jnl. Mech. Engrg. Sci., Institution of Mech. Engrs., London, Vol. 11, No. 3, June 1969, pp. 234-242.

1970

- [2.15] Davenport, A.G., et al.: "A Study of Wind Action on a Suspension Bridge During Erection and on Completion -- Appendix," BLWT-4-70, Boundary Layer Wind Tunnel Laboratory, Univ. of Western Ontario, London, Canada, March 1970.

1971

- [2.16] Scanlan, R.H. and Tomko, J.J.: "Airfoil and Bridge Deck Flutter Derivatives," Jnl. Eng. Mech. Div. Proc. Amer. Soc. Div. Eng., Vol. 97, No. EM6, Dec. 1-71, pp. 1717-1737.

- [2.17] Simiu, E.: "Buffeting and Aerodynamic Stability of Suspension Bridges in Turbulent Wind," Doctoral Dissertation, Princeton University, May 1971.
- [2.18] Standen, N.M., Dalglish, W.A., Templin, R.J.: "A Wind Tunnel and Full-Scale Study of Turbulent Wind Pressures on a Tall Building," Proc. Int'l Conf. on Wind Effects on Bldgs. & Struct., Tokyo, 1971, Paper II.3-1 to 3-11.

1973

- [2.19] Coupry, G." "Random Techniques for Flutter Testing in Wind Tunnel and in Flight," Israel Jnl. of Technology, Vol. 11, Nos. 1-2, 1973, pp. 33-39.

1974

- [2.20] Beliveau, J.G., Vaicaitis, R., Shinozuka, M.: "Motion of a Suspension Bridge Subject to Wind Loads," Paper, ASCE-EMD Specialty Conf. on Probabilistic Methods, Stanford Univ., June 1974.
- [2.21] Sabzevari, A. and Hjorth-Hansen, E.: "On Improving the Aerodynamic Stability of H and Channel Sections," Publications, International Assn. for Bridge and Struc. Eng., Vol. 34-I, pp. 129-144.

1975

- [2.22] Holmes, J.D.: "Prediction of the Response of a Cable-Stayed Bridge to Turbulence," Proc. 4th Int'l. Conf. on Wind Effects on Bldgs. and Structures, London, Sept. 1975.
- [2.23] Konishi, I., Shiraishi, N., Matsumoto, M., and Okanan, H.: "Fundamental Consideration on the Aerodynamic Admittance of Long-Spanned Bridges," Annual Report No. 18, Disaster Prevention Research Institute, Kyoto University, 1975, pp. 395-413. (in Japanese)
- [2.24] Konishi, I., Shiraishi, N., and Matsumoto, M.: "Aerodynamic Response Characteristics of Bridge Structures," Proc. 4th Int. Conf. on Wind Effects on Bldgs. and Structures, London, U.K., Sept. 1975, pp. 199-208.
- [2.25] Loiseau, H., and Széchenyi, E.: "Étude du Comportement Aéroelastique du Tablier d'un Pont à Haubans," T.P. 1975-75, Office National d'Études et de Recherches Aérospatiales, Châtillon, France.
- [2.26] Miyata, T., Kubo, Y. and Ito, M.: "Analysis of Aeroelastic Oscillations of Long-Span Structures by Nonlinear Multi-dimensional Procedures," Proc. 4th Int. Conf. on Wind Effects on Bldgs. and Structures, London, U.K., Sept. 1975, pp. 215-225.

[1975] cont.

- [2.27] Otsuki, Y., Washizu, K., Ohya, A.: "Wind Tunnel Experiments on the Aeroelastic Instability of a Prismatic Model with a Rectangular Section," 75-AM, JSME A-15, Proceedings, Joint JSME-ASME Applied Mechanics Western Conference, Honolulu, Hawaii, March 24-27, 1975, pp. 145-152.
- [2.28] Okubo, T., Narita, N., Yokoyama, K.: "On the Wind Response of the Kanmon Bridge," Paper presented at the Seventh Joint Meeting, UJNR, 20-23, May 1975, Tokyo, Japan.
- [2.29] Scanlan, R.H.: "Recent Methods in the Application of Test Results to the Wind Design of Long, Suspended-Span Bridges," Report No. FHWA-RD-75-115, Federal Highway Admin., Office of Research and Development, Washington, D.C., 1975.

1976

- [2.30] Chi, M.: "Response of Bridge Structural Members under Wind-Induced Vibrations," Report FHWA-RD-78-25, Federal Highway Admin., ORD, DOT, Washington, D.C. 20590, June 1976.
- [2.31] Gade, R.H., Bosch, H.R., and Podolny, W. Jr.: "Recent Aerodynamic Studies of Long-Span Bridges," Jn. Struct. Div., ASCE, Vol. 102, No. ST 7, July 1976, pp. 1299-1315.
- [2.32] Irwin, H.P.A.H., and Wardlaw, R.L.: "Sectional Model Experiments on Lions' Gate Bridge, Vancouver," Laboratory Technical Report No. LTR-LA-205, National Research Council, Ottawa, Canada, October 1976.
- [2.33] Miyata, T. and Tanaka, H.: "Aerodynamics of Long-Span Structures," Wind Effects on Structures, Univ. of Tokyo Press, Tokyo, Japan, 1976, pp. 245-256.
- [2.34] Okauchi, I., et al.: "The Wind Resistant Experimental Bridge for the Honshu-Shikoku Island Link-Bridge," Research Report, Commission of the Honshu-Shikoku Island Link-bridge Corp. (in Japanese) 1976.
- [2.35] Shinozuka, M., Imai, H., Enami, Y., and Takemura, K.: "Identification of Aerodynamic Characteristics of a Suspension Bridge Based on Field Data," Paper presented at IUTAM Symposium on Stochastic Problems in Dynamics, Southampton, England, July 19-23, 1976.

1977

- [2.36] Chi, M., Neal, E., and Dennis, B.G. Jr.: "Determination of Strouhal Characteristics and Power Spectrum for Elastically Restrained H-Shape Sections," Report FHWA-RD-78-26, Federal Highway Administration, ORD, DOT, Washington, DC, 20590, Aug. 1977.

[1977] cont.

- [2.37] Gade, R.H., and Bosch, H.R.: "Aerodynamic Investigations of the Luling, Louisiana Cable-Stayed Bridge," Office of Research and Development, FHWA, DOT, Oct. 1977.
- [2.38] Hjorth-Hansen, E.: "Model Tests on Flow-Induced Vibrations of Bridge Decks of the Channel Type," Jn. Indust. Aerodyn., Amsterdam, Vol. 2, 1977, pp. 113-128.
- [2.39] Hjorth-Hansen, E.: "Regular Drag Fluctuations Due to Air Flow Normal to a Plate-Type Structure," Jn. of Indust. Aerodyn., Amsterdam, Vol. 2, 1977, pp. 129-132.
- [2.40] Irwin, H.P.A.H.: "A Wind Tunnel Investigation of the Proposed St. John's River Bridge, Jacksonville, Florida," Laboratory Technical Report, LTR-LA-212, National Research Council, Ottawa, Canada, January 1977.
- [2.41] Irwin, H.P.A.H.: "Wind Tunnel and Analytical Investigations of the Response of Lions' Gate Bridge to a Turbulent Wind," Laboratory Technical Report, LTR-LA-210, National Research Council, Ottawa, Canada, June 1977.
- [2.42] Irwin, H.P.A.H. and Schuyler, G.D. "Experiments on a Full Aero-elastic Model of Lions' Gate Bridge in Smooth and Turbulent Flow," Laboratory Technical Report, LTR-LA-206, National Research Council, Ottawa, Canada, 18 Oct. 1977.
- [2.43] Scanlan, R.H. and Gade, R.H.: "Motion of Suspended Bridge Spans Under Gusty Wind," Jn. of the Structural Division, ASCE, Vol. 103, No. ST 9, Sept. 1977, pp. 1867-1883.
- [2.44] Shinozuka, M. et al: "Identification of Aerodynamic Characteristics of a Suspension Bridge Based on Field Data," Stochastic Problems in Dynamics, B.L. Clarkson (Ed.), Pitman, San Francisco and London, 1977, pp. 214-236.
- [2.45] Shiraishi, N. and Matsumoto, M.: "Aerodynamic Responses of Bridge Structures Subjected to Strong Winds," Proc. Sympos. on Engrg. for Natural Hazards, Manila, Sept. 1977.
- [2.46] Teunissen, H.W.: "A Measurement and Analysis Facility for Full-Scale Atmospheric Wind and Turbulence Data," Internal Report No. MSRB-77-2, Atmospheric Environment Service, Downsview, Ont., Canada, July 1977.

1978

- [2.47] Cook, N.J.: "Wind-Tunnel Simulation of the Adiabatic Atmospheric Boundary Layer by Roughness, Barrier and Mixing-Device Methods," Jn. of Indust. Aerodyn., Amsterdam, Vol. 3, 1978, pp. 157-176.

[1978] cont.

- [2.48] Dowell, E.H., Sisto, F., Curtiss, H.C. Jr. and Scanlan, R.H.: A Modern Course in Aeroelasticity, Sijthoff and Nordhoff, Amsterdam, 1978.
- [2.49] Holmes, J.D.: "Monte Carlo Simulation of the Wind-Induced Response of a Cable-Stayed Bridge," Wind Engineering Report 2/78, Dept. of Civil & Systems Engineering, James Cook University of North Queensland, Australia, June 1978.
- [2.50] Irwin, H.P.A.H. et al: "A Wind Tunnel Investigation of a Steel Design for the St. Johns River Bridge, Jacksonville, Florida," Laboratory Technical Report, LTR-LA-220, National Research Council, Ottawa, Canada, February, 1978.
- [2.51] Irwin, H.P.A.H. and Schyler, G.D.: "Wind Effects on a Full Aeroelastic Bridge Model," Preprint No. 3268, ASCE Spring Convention and Exhibit, Pittsburgh, Pa., April 24-28, 1978.
- [2.52] Irwin, H.P.A.H.: "Further Investigations of a Full Aeroelastic Model of Lions' Gate Bridge," Laboratory Technical Report, LTR-LA-221, National Research Council, Ottawa, Canada, May 1978.
- [2.53] Jensen, N.O. and Hjorth-Hansen, E.: "Turbulence and Response Measurements at Sotra Bridge," SINTEF, Report No. STF 71-A78003, Univ. of Trondheim, Norway, Feb. 1978.
- [2.54] Simiu, E. and Scanlan, R.H., Wind Effects on Structures, Wiley, New York, N.Y., 1978.
- [2.55] Scanlan, R.H.: "The Action of Flexible Bridges Under Wind. I: Flutter Theory, II: Buffeting Theory," Jn. of Sound and Vibration, Vol. 60, No. 2, 1978, pp. 187-199 and (II) pp. 201-211.
- [2.56] Széchenyi, E. and Loiseau, H.: "Mesures Aérodynamiques et Dynamiques sur le Pont de Saint-Nazaire," T.P. No. 1978-26, ONERA, 1978.
- [2.57] Széchenyi, E. and Tourjansky, N.: "Stabilité Aéroélastique des Ponts Suspendus à Haubans," T.P. No. 1978-27, ONERA, 1978.
- [2.58] Wardlaw, R.L.: "Sectional Versus Full Model Wind Tunnel Testing of Bridge Road Decks," DME/NAE Quarterly Bulletin, NO. 1978(4), pp. 25-47.
- [2.59] Williams, C.D., Teunissen, H.W., Irwin, H.P.A.H.: "The Lions' Gate Bridge -- Wind Measurements and Wind Tunnel Investigations," Proc. Second Canadian Workshop on Wind Engineering, Varennes, Quebec, Sept. 28-29, 1978, pp. 179-183.

1979

- [2.60] Grilaud, G.: "Les Methodes d'etude aérodynamique sur les ponts Suspendus ou à Haubans," Report No. EN. ADYM 79-6-R, Centre Scientifique et Technique du Batiment, Nantes, France.
- [2.61] Irwin, H.P.A.H.: "Centre of Rotation for Torsional Vibration of Bridges," Jn. of Indust. Aerodyn., Vol. 4, No. 2, March 1979, pp. 123-132.
- [2.62] Teunissen, H.W.: "Measurements of Planetary Boundary Layer Wind and Turbulence Characteristics over a Small Suburban Airport," Jn. of Indust. Aerodyn., Vol. 4, 1979, pp. 1-34, Amsterdam.
- [2.63] Scanlan, Robert H.: "On the State of STability Considerations for Suspended-Span Bridges Under Wind," Proc. Symposium on Practical Experiences with Flow-Induced Vibrations, Univ. of Karlsruhe, Germany, Sept. 1979 (in press).
- [2.64] Melbourne, W.H.: "Model and Full Scale Response to Wind Action of the Cable Stayed Box Girder West Gate Bridge," Proceedings, Symposium on Practical Experiences with Flow-Induced Vibrations, Karlsruhe, Sept. 1979 (in press).

III. ANALYTICS OF THE FLUTTER PROBLEM

Refs. [3.1], [3.2],* treat this problem in detail. The aim of the present presentation will be to guide the designer to those minimum essential steps necessary for design. Unusual or special considerations will be omitted.

3.1 The 2-D Problem

Consider the bridge deck section as pictured in Fig. 3.1. Let h represent the vertical deflection of the local c.g. of the section and α the rotation coordinate (angle) about that c.g.. Let m represent the mass per unit span and I , the mass moment of inertial about the c.g., per unit span. Then (neglecting lateral motion as unimportant to flutter) the two sectional equations of motion are

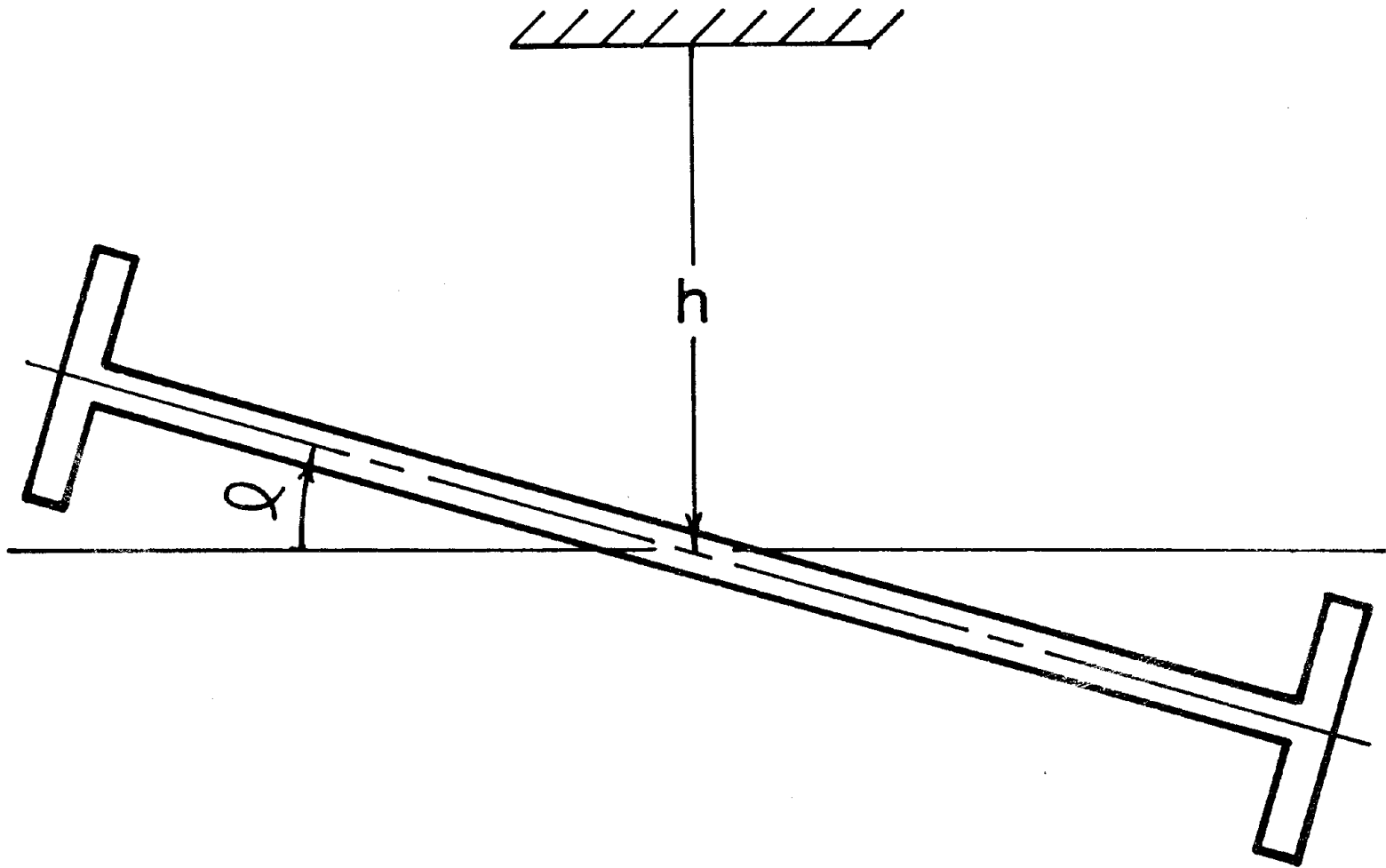
$$(3.1a) \quad M[\ddot{h} + 2 \zeta_h \omega_h \dot{h} + \omega_h^2 h] = L_h$$

$$(3.1b) \quad I[\ddot{\alpha} + 2 \zeta_\alpha \omega_\alpha \dot{\alpha} + \omega_\alpha^2 \alpha] = M_\alpha$$

where ζ_h, ζ_α are the damping ratios-to-critical and ω_h, ω_α are the natural circular frequencies, respectively in h - and α - motions, and L_h, M_α are the aerodynamic force and moment per unit span acting on the section.

The above equations (3.1a and b) are written for a bridge deck section that is horizontally balanced about its c.g. If this is not the case, but the deck is unbalanced instead, i.e., is unsymmetrical about

* Numbers in brackets refer to the listing at the end of Section III.



DEGREES OF FREEDOM FOR DECK SECTION

FIGURE 3.1

its c.g.), the corresponding equations become

$$(3.2a) \quad m[\ddot{h} + a \ddot{\alpha} + 2 \zeta_h \omega_h \dot{h} + \omega_h^2 h] = L_h$$

$$(3.2b) \quad I[\ddot{\alpha} + \frac{a}{r_g} \ddot{h} + 2 \zeta_\alpha \omega_\alpha \dot{\alpha} + \omega_\alpha^2 \alpha] = M_\alpha$$

where ma is the mass unbalance of the section about its c.g., and r_g is its radius of gyration about the same point.

The aerodynamic force and moment at the c.g. are of the linear, self-excited type and are basically given by

$$(3.3a) \quad L_h = H_1 \dot{h} + H_2 \dot{\alpha} + H_3 \alpha$$

$$(3.3b) \quad M_\alpha = A_1 \dot{h} + A_2 \dot{\alpha} + A_3 \alpha$$

where the coefficients H_i, A_i ($i=1,2,3$) are aerodynamic in origin and must be determined experimentally for the particular shape of deck in question.

The coefficients H_1 , pertaining to h , and A_2 and A_3 , pertaining to $\dot{\alpha}$ and α , are the direct coefficients, and the others (H_2, H_3 , and A_1) are the coupling coefficients. In many instances, the direct coefficients prove to be the more important.

By their nature, the coefficients H_i and A_i are dimensional, and a nondimensional form for them is needed so that their values, determined in scaled model experiments, can be transferred for use in full

scale. This is done [3.3] by writing eqs.(3.3) in the form

$$(3.3c) \quad L_h = \frac{1}{2} \rho U^2 (2B) \left[K H_1^* \frac{\dot{h}}{U} + K H_2^* \frac{B\dot{\alpha}}{U} + K^2 H_3^* \alpha \right]$$

$$(3.3d) \quad M_\alpha = \frac{1}{2} \rho U^2 (2B^2) \left[K A_1^* \frac{\dot{h}}{U} + K A_2^* \frac{B\dot{\alpha}}{U} + K^2 A_3^* \alpha \right]$$

where

$$\rho = \text{air density} \quad \left\{ \begin{array}{l} \rho = 0.002378 \text{ slugs/ft}^3 \\ \rho = 1.228 \text{ kg/m}^3 = 1.228 \times 10^{-3} \text{ gm/cm}^3 \end{array} \right.$$

U = cross wind velocity

$$K = \frac{B\omega}{U}$$

B = deck width

ω = circular frequency of flutter oscillation

and the nondimensional aerodynamic coefficients H_i^* and A_i^* bear the following relation to H_i and A_i :

$$(3.4) \quad \left\{ \begin{array}{l} H_1^* = \frac{m H_1}{\rho B^2 \omega} ; \\ H_2^* = \frac{m H_2}{\rho B^3 \omega} ; \\ H_3^* = \frac{m H_3}{\rho B^3 \omega^2} ; \end{array} \right. \quad \left\{ \begin{array}{l} A_1^* = \frac{I A_1}{\rho B^3 \omega} \\ A_2^* = \frac{I A_2}{\rho B^4 \omega} \\ A_3^* = \frac{I A_3}{\rho B^4 \omega^2} \end{array} \right.$$

Some examples of the values experimentally obtained for H_i^* and A_i^* are illustrated in Figs. 3.2 and 3.3 for decks whose sectional form is sketched on the figures. The plots are given as functions of $\frac{U}{NB} = \frac{2\pi}{K}$.

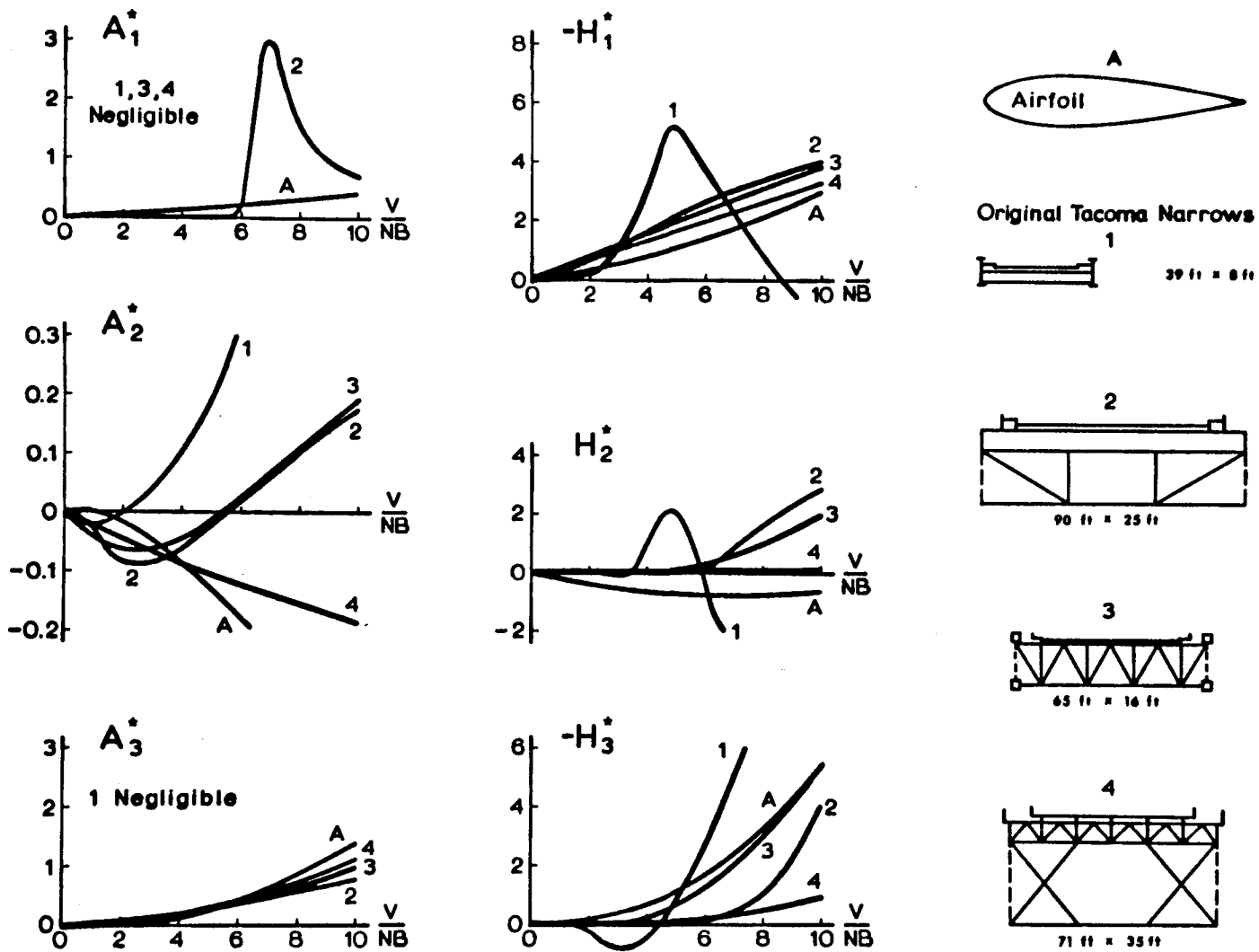


FIGURE 3.2

AERODYNAMIC COEFFICIENTS

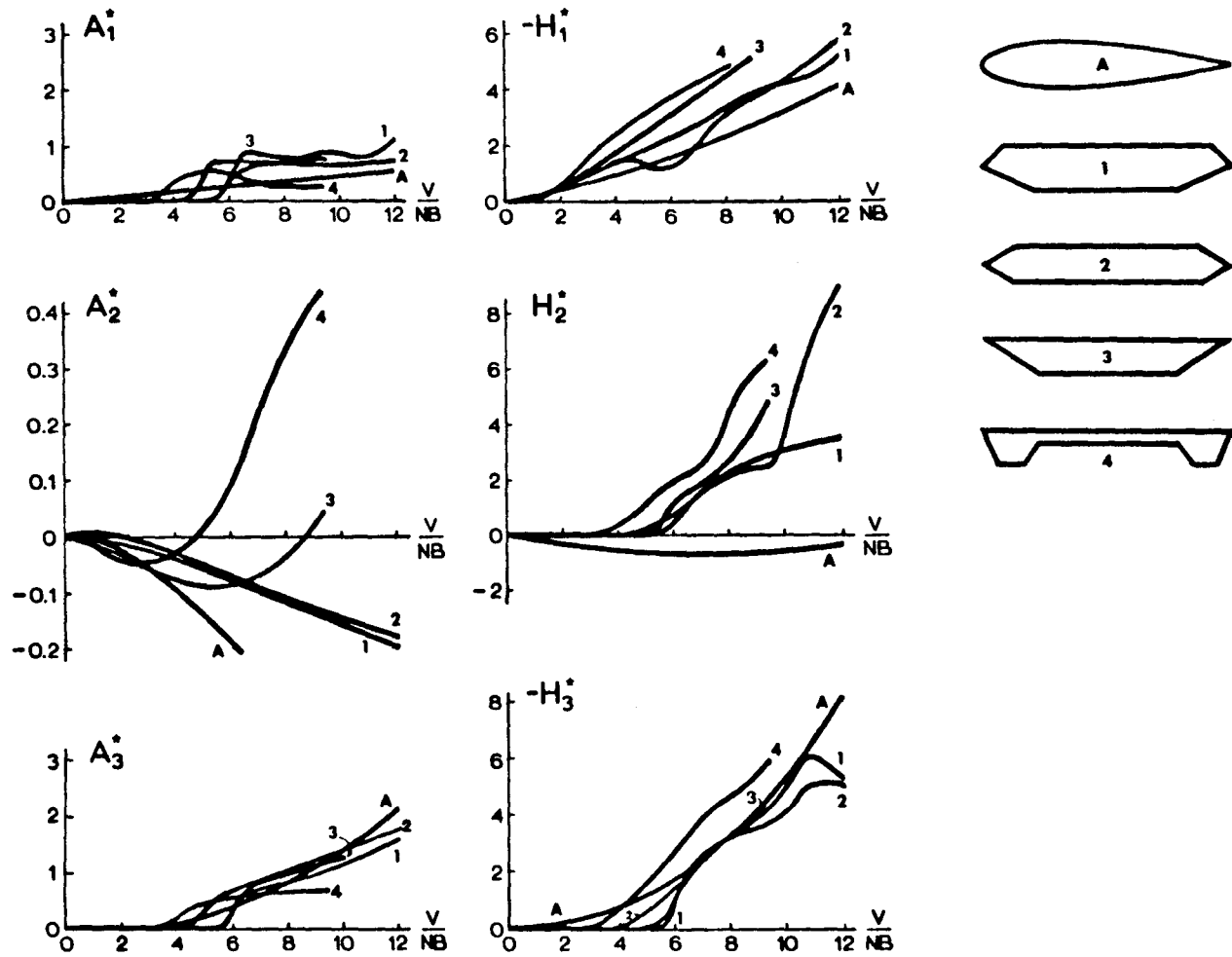


FIGURE 3.3

AERODYNAMIC COEFFICIENTS

It should be noted that the products KH_1^* , KA_1^* , etc., play the roles of flutter derivatives. Consider the term $H_1 \dot{h}$, for example. This has the dimension of a force per unit span length. If written in classic aerodynamic lift force form, it would have the appearance

$$\frac{1}{2} \rho U^2 (2B) KH_1^* \frac{\dot{h}}{U} = H_1 \dot{h} = \frac{1}{2} \rho U^2 (2B) C_L \approx \frac{1}{2} \rho U^2 (2B) \frac{dC_L}{d\bar{\alpha}} \frac{\dot{h}}{U}$$

where $\bar{\alpha} = \frac{\dot{h}}{U}$ is an "effective" angle of attack.

Thus,

$$KH_1^* = \frac{dC_L}{d\bar{\alpha}}$$

where $dC_L/d\bar{\alpha}$ is the derivative of a lift coefficient C_L with respect to angle of attack.

It is emphasized again that the values of all the aerodynamic derivatives must be experimentally obtained, and they evolve as functions of reduced velocity U/NB . Of particular interest is the manner in which the coefficient A_2^* evolves with U/NB . This coefficient is proportional to torsional aerodynamic damping, and it plays a central role in many cases of bridge flutter susceptibility, since it often changes sign (from stable to unstable) with increasing U/NB in certain cases.

3.2 The 3-D Problem

3.2.1 Case of the Straight Horizontal Deck

To proceed from analysis of the spanwise deck section to the full span, let $h(x,t)$, $\alpha(x,t)$ represent h and α values as function of

the spanwise position x and time t . It will be assumed in this case, that bending and torsion modes of the bridge are independent (uncoupled) from each other. Let $h(x)$ be the modal deflection form in the lowest bending mode and $\alpha(x)$ be the modal deflection form in the lowest torsional mode. Then,

$$h(x,t) = h(x) p(t)$$

$$\alpha(x,t) = \alpha(x) q(t)$$

where p and q are now the generalized coordinates. The equations of motion (3.1) for the balanced deck then convert immediately to

$$(3.5a) \quad M_1 [\ddot{p} + 2 \zeta_h \omega_h \dot{p} + \omega_h^2 p] = \frac{1}{2} \rho U^2 (2B) [KC_{11} H_1^* \frac{\dot{p}}{U} + KC_{12} H_2^* \frac{B \dot{q}}{U} + K^2 C_{12} H_3^* q]$$

$$(3.5b) \quad I_1 [\ddot{q} + 2 \zeta_\alpha \omega_\alpha \dot{q} + \omega_\alpha^2 q] = \frac{1}{2} \rho U^2 (2B^2) [KC_{12} A_1^* \frac{\dot{p}}{U} + KC_{22} A_2^* \frac{B \dot{q}}{U} + K^2 C_{22} A_3^* q]$$

where

$$(3.6a) \quad M_1 = \int_{\text{span}} m(x) h^2(x) dx$$

$$(3.6b) \quad I_1 = \int_{\text{span}} I(x) \alpha^2(x) dx$$

$$(3.6c) \quad C_{11} = \int_{\text{span}} h^2(x) dx$$

$$(3.6d) \quad C_{12} = \int_{\text{span}} h(x) \alpha(x) dx$$

$$(3.6e) \quad C_{22} = \int_{\text{span}} \alpha^2(x) dx$$

are generalized mass, moment of inertia, and modal factors, respectively. Generalizations of Eqs. (3.2) for the unbalanced deck are direct but will be omitted here. Note that \int_{span} represents an integral over the entire side- and main-spans of the bridge (i.e. over whatever constitutes the mode in question).

3.3 Case of an Arched or Curved Deck

When the deck of the bridge is curved in either the vertical or the horizontal plane, coupling of bending, torsional and lateral deflections occurs in all natural modes; in other words, each mode consists, at any given spanwise station, of vertical, torsional, and lateral deflection components of the local c.g. of the deck section.

Including then a lateral or sway deflection r of the deck c.g. at spanwise section x , the vertical, torsional, and lateral deflections in the first two natural modes may be expressed as

$$(3.7a) \quad \frac{h(x,t)}{B} = h_1(x) \xi_1(t) + h_2(x) \xi_2(t)$$

$$(3.7b) \quad \alpha(x,t) = \alpha_1(x) \xi_1(t) + \alpha_2(x) \xi_2(t)$$

$$(3.7c) \quad \frac{r(x,t)}{B} = r_1(x) \xi_1(t) + r_2(x) \xi_2(t)$$

where $h_i(x)$, $\alpha_i(x)$, $r_i(x)$ ($i=1,2$) are the dimensionless modal form components associated with the i^{th} mode, and $\xi_i(t)$ ($i=1,2$) are the associated dimensionless generalized coordinates.

The total kinetic energy of the system is the spanwise integrated sum of displacement and rotational energies:

$$(3.8) \quad T = \frac{1}{2} \int_{\text{span}} \{m(x)[\dot{h}^2(x,t) + \dot{r}^2(x,t)] + I(x) \dot{\alpha}^2(x,t)\} dx$$

where $m(x)$ and $I(x)$ are the mass and mass moment of inertia per unit length of the deck and associated cables per unit span. Under the generalized orthogonality condition

$$(3.9) \quad \int_{\text{span}} \{m(x)[h_i(x)h_j(x) + r_i(x)r_j(x)] B^2 + I(x) \alpha_1(x) \alpha_2(x)\} dx = 0$$

(i ≠ j)

The kinetic and potential energies of the system may be written:

$$(3.10) \quad T = \frac{1}{2} \{I_1 \dot{\xi}_1^2 + I_2 \dot{\xi}_2^2\}$$

$$(3.11) \quad U = \frac{1}{2} \{\omega_1^2 I_1 \xi_1^2 + \omega_2^2 I_2 \xi_2^2\}$$

where, for $i=1$ or 2 :

$$(3.12) \quad I_i = \int_{\text{span}} \{m(x)[h_i^2(x) + r_i^2(x)] B^2 + I(x) \alpha_i^2(x)\} dx$$

I_i being the generalized inertia in the i^{th} mode and ω_i being its natural circular frequency.

Under the conditions described, and with the inclusion of assigned damping ratios ζ_i to the respective modes, the equations of motion become

$$(3.13a) \quad I_i[\ddot{\xi}_1 + 2\zeta_1\omega_1\dot{\xi}_1 + \omega_1^2\xi_1] = Q_1$$

$$(3.13b) \quad I_2[\ddot{\xi}_2 + 2\zeta_2\omega_2\dot{\xi}_2 + \omega_2^2\xi_2] = Q_2$$

the Q_i being the generalized forces. Employing the basic section aerodynamic (self-excited) force expressions (3.3), with h and α as in (3.7), the generalized forces, at the circular flutter frequency ω , can be found to be

$$(3.14a) \quad Q_1 = \rho U^2 B^4 \left\{ \frac{K H_1^*}{U} (C_{h_1 h_1} \dot{\xi}_1 + C_{h_1 h_2} \dot{\xi}_2) + \frac{K H_2^*}{U} (C_{h_1 \alpha_1} \dot{\xi}_1 + C_{h_1 \alpha_2} \dot{\xi}_2) \right. \\ \left. + \frac{K^2 H_3^*}{B} (C_{h_1 \alpha_1} \xi_1 + C_{h_1 \alpha_2} \xi_2) \right. \\ \left. + \frac{K A_1^*}{U} (C_{h_1 \alpha_1} \dot{\xi}_1 + C_{h_2 \alpha_1} \dot{\xi}_2) + \frac{K A_2^*}{U} (C_{\alpha_1 \alpha_1} \dot{\xi}_1 + C_{\alpha_1 \alpha_2} \dot{\xi}_2) \right. \\ \left. + \frac{K^2 A_3^*}{U} (C_{\alpha_1 \alpha_1} \xi_1 + C_{\alpha_1 \alpha_2} \xi_2) \right\}$$

$$\begin{aligned}
(3.14b) \quad Q_2 = \rho U^2 B^4 & \left\{ \frac{K H_1^*}{U} [(C_{h_1 h_2} \dot{\xi}_1 + C_{h_2 h_2} \dot{\xi}_2) + \frac{K H_2^*}{U} (C_{h_2 \alpha_1} \dot{\xi}_1 + C_{h_2 \alpha_2} \dot{\xi}_2) \right. \\
& + \frac{K^2 H_3^*}{B} (C_{h_2 \alpha_1} \xi_1 + C_{h_2 \alpha_2} \xi_2) \\
& + \frac{K A_1^*}{U} (C_{h_1 \alpha_2} \dot{\xi}_1 + C_{h_2 \alpha_2} \dot{\xi}_2) + \frac{K A_2^*}{U} (C_{\alpha_1 \alpha_2} \dot{\xi}_1 + C_{\alpha_2 \alpha_2} \dot{\xi}_2) \\
& \left. + \frac{K^2 A_3^*}{B} (C_{\alpha_1 \alpha_2} \xi_1 + C_{\alpha_2 \alpha_2} \xi_2) \right\}
\end{aligned}$$

where

$$(3.15) \quad C_{a_i b_j} = \int_{\text{span}} a_i b_j \frac{dx}{B}$$

in which (a,b) range over (h, α), and (i,j) range over (1,2).

There are 10 such coefficients of interest here.

The generalized forces may further be reduced to the form

$$(3.16a) \quad Q_1 = \rho B^5 \omega \{ E_{11}(K) \dot{\xi}_1 + \omega F_{11}(K) \xi_1 + E_{12}(K) \dot{\xi}_2 + \omega F_{12}(K) \xi_2 \}$$

$$(3.16b) \quad Q_2 = \rho B^5 \omega \{ E_{21}(K) \dot{\xi}_1 + \omega F_{21}(K) \xi_1 + E_{22}(K) \dot{\xi}_2 + \omega F_{22}(K) \xi_2 \}$$

where

$$(3.17a) \quad E_{11}(K) = H_1^*(K) C_{h_1 h_1} + H_2^*(K) C_{h_1 \alpha_1} + A_1^*(K) C_{h_1 \alpha_1} + A_2^*(K) C_{\alpha_1 \alpha_1}$$

$$(3.17b) \quad E_{12}(K) = H_1^*(K) C_{h_1 h_2} + H_2^*(K) C_{h_1 \alpha_2} + A_1^*(K) C_{h_2 \alpha_1} + A_2^*(K) C_{\alpha_1 \alpha_2}$$

$$(3.17c) \quad E_{21}(K) = H_1^*(K)C_{h_1 h_2} + H_2^*(K)C_{h_2 \alpha_1} + A_1^*(K)C_{h_1 \alpha_2} + A_2^*(K)C_{\alpha_1 \alpha_2}$$

$$(3.17d) \quad E_{22}(K) = H_1^*(K)C_{h_2 h_2} + H_2^*(K)C_{h_2 \alpha_2} + A_1^*(K)C_{h_2 \alpha_2} + A_2^*(K)C_{\alpha_2 \alpha_2}$$

$$(3.18a) \quad F_{11}(K) = H_3^*(K)C_{h_1 \alpha_1} + A_3^*(K)C_{\alpha_1 \alpha_1}$$

$$(3.18b) \quad F_{12}(K) = H_3^*(K)C_{h_1 \alpha_2} + A_3^*(K)C_{\alpha_1 \alpha_2}$$

$$(3.18c) \quad F_{21}(K) = H_3^*(K)C_{h_2 \alpha_1} + A_3^*(K)C_{\alpha_1 \alpha_2}$$

$$(3.18d) \quad F_{22}(K) = H_3^*(K)C_{h_2 \alpha_2} + A_3^*(K)C_{\alpha_2 \alpha_2}$$

It is seen from the form of the generalized forces (3.23) that the equations of motion (3.20) are coupled together by the aerodynamic forces, the degree of coupling depending on both the aerodynamic flutter derivatives and the modal cross-coupling coefficients (3.15).

3.4 Solutions of the Flutter Equations

3.4.1 Simplest Case: Pure Torsional Flutter

(or any coupled flutter in which torsion alone becomes unstable)

If the torsional coefficient A_2^* reverses sign with increasing $\frac{U}{NB}$ (see, for example, Fig. 3.4), flutter instability is indicated. This is, in fact, a very common case in practice. To find the wind velocity at flutter ("critical flutter velocity"), proceed as follows.

In Eq. (3.5b), consider only the damping terms (proportional to \dot{q}). Mechanical damping is just balanced out by aerodynamic damping if:

$$(3.19) \quad I_1(2\zeta_\alpha \omega_\alpha) \dot{q} = \rho U^2 B^2 K C_{22} A_2^* \frac{B \dot{q}}{U}$$

Assuming (as is usually the case), that flutter occurs practically at the same frequency as the first mode, let $\omega \cong \omega_\alpha$. Then the condition (3.19) yields the critical value of A_2^* as

$$(3.20) \quad A_2^* \cong \frac{2 I_1 \zeta_\alpha}{\rho B^4 C_{22}}$$

(In effect, this states that the critical flutter value of A_2^* is equal to the "scaled" value of mechanical damping ζ_α in the α -mode by a factor equal to twice the ratio of the generalized mechanical inertia to the generalized aerodynamic inertia.)

The corresponding value $(U/NB)_c$, is the critical one, and the critical wind velocity is

$$(3.2) \quad U_c = NB \left(\frac{U}{NB} \right)_c$$

Note: If A_2^* never changes sign, the critical flutter velocity may be high, but in any case, it depends upon solution of the two-degree-of-freedom problem (in both p and q). This is treated below.

3.4.2 The Two-Degree-of-Freedom Case for Straight Decks

This case is more rare and likely to produce flutter only if the lowest bending and torsion frequencies of the bridge are "near" each other. Further, it will not be the important case for a design unless the plot of the coefficient A_2^* does not reverse sign.

When the conditions for two-degree flutter are satisfied (as, occasionally, for very streamlined bridges), the flutter that can occur is said to be of the "classical" airfoil, or "coupled" type. This is a flutter in which interaction of aerodynamic stiffness terms, rather than damping terms, is the principal mechanism.

The solution proceeds by assuming a sinusoidal response jointly in p and q and setting the determinant of the two-equation system (3.5) equal to zero. Details are given in Ref. [3.2]. Letting

$$(3.22) \quad X = \omega/\omega_h$$

where ω is the circular flutter frequency, the following two simultaneous equations, with X as unknown, are obtained:

$$(3.23a) \quad a_4 X^4 + a_3 X^3 + a_2 X^2 + a_1 X + a_0 = 0$$

$$(3.23b) \quad b_3 X^3 + b_2 X^2 + b_1 X + b_0 = 0$$

where the coefficients a_i and b_i are the following constants or functions of K :

$$(3.24a) \quad a_0 = \left(\frac{\omega_\alpha}{\omega_h}\right)^2$$

$$(3.24b) \quad a_1 = 0$$

$$(3.24c) \quad a_2 = \frac{\omega_\alpha^2}{\omega_h^2} - 4\zeta_h \zeta_\alpha \frac{\omega_\alpha}{\omega_h} - 1 - \frac{\rho B^4}{I_1} C_{22} A_3^*$$

$$(3.24d) \quad a_3 = 2\zeta_\alpha \frac{\omega_\alpha}{\omega_h} \frac{\rho B^2}{M_1} C_{11} H_1^* + 2\zeta_h \frac{\rho B^4}{I_1} C_{22} A_2^*$$

$$(3.24e) \quad a_4 = 1 + \frac{\rho B^4}{I_1} C_{22} A_3^* + \frac{\rho B^2}{M_1} \frac{\rho B^4}{M_1} (C_{12}^2 A_1^* H_2^* - C_{11} C_{22} A_2^* H_1^*)$$

$$(3.25a) \quad b_0 = 2\zeta_h \left(\frac{\omega_\alpha}{\omega_h}\right)^2 + 2\zeta_\alpha \frac{\omega_\alpha}{\omega_h}$$

$$(3.25b) \quad b_1 = -\frac{\rho B^2}{M_1} C_{11} H_1^* \frac{\omega_\alpha^2}{\omega_h^2} - \frac{\rho B^4}{I_1} C_{22} A_2^*$$

$$(3.25c) \quad b_2 = -2\zeta_\alpha \frac{\omega_\alpha}{\omega_h} - 2\zeta_h - 2\zeta_h \frac{\rho B^4}{I_1} C_{22} A_3^*$$

$$(3.25d) \quad b_3 = \frac{\rho B^4}{I_1} C_{22} A_2^* + \frac{\rho B^2}{M_1} C_{11} H_1^* \frac{\rho B^2}{M_1} \frac{\rho B^4}{I_1} (C_{11} C_{22} H_1^* A_3^* - C_{12}^2 A_1^* H_3^*)$$

The solution method is as follows. A value of K is chosen and all the coefficients H_i^* and A_i^* are evaluated for that K . Then a_i and b_i in (3.12) and (3.13) are evaluated. These constants are then used in Eqs. (3.11). Eqs. (3.11) are then solved for the values of X corresponding to the K chosen. The above process is repeated for a series of values of K .

Plots of the solutions X of (3.23a) and (3.23b) are made vs. the K values used. Where the plot of solutions X for (3.23a) crosses the plot of solutions X from (3.23b), the critical flutter condition X_c exists. The corresponding K value is

$$K_c = \frac{B \omega_h X_c}{U_c}$$

i.e., the critical flutter velocity is

$$(3.26) \quad U_c = \frac{B \omega_h X_c}{K_c}$$

Example of Pure Torsional Flutter

Consider the case where coefficient A_2^* is the only important torsional aerodynamic coefficient, as given, for example, by Fig. 3.2, Bridge 2. Let the bridge deck mass moment of inertia per unit span be

$$I = 857,000 \text{ lb. sec}^2 (3.9 \times 10^5 \text{ kg sec}^2)$$

with $B = 100 \text{ ft}$ (30.5 meters). If the deck is uniform, $I_1 = C_{22} I$ and, according to eq. (3.20), the critical value of A_2^* is given by

$$(A_2^*)_{\text{crit}} = \frac{2 I \zeta_\alpha}{\rho B^4}$$

For a value of mechanical damping of $\zeta = 0.01$ and air at sea level density

$$(A_2^*)_{\text{crit}} = \frac{2.857000 \cdot (0.01)}{(0.002378) \cdot 100^4} = 0.072 \quad (\text{nondimensional})$$

According to Fig. 3.2 this corresponds to a critical U/NB value of 7.1 which, for a natural torsional frequency of $N=0.2 \text{ Hz}$, corresponds to a flutter velocity of $U_c = 142 \text{ ft/sec} = 96.8 \text{ mph} (= 156 \text{ km/hr})$.

Example of Two-Degree Flutter

The mechanical damping ζ_r and ζ_h will both be taken as 0.01; the aerodynamic coefficients will be taken from Fig. 3.3 and are as listed below (for bridge section #2). The deck width $B=100$ ft (30.5m), while the span $L = 4,000$ ft. (1220 m). The vertical and torsional modes will be assumed to be half sine waves, therefore $C_{11} = C_{12} = C_{22} = L/2 = 2,000$ ft. (610 m). The constant sectional moment of inertia per unit span will be taken as $I = 857,000$ lb. sec² (3.9×10^5 kg sec²) while the mass of the deck per unit span will be $M = 711.8$ lb sec²/ft² (3481 kg sec²/m²). These lead to:

$$\left(\frac{\rho B^4}{I_1}\right)C_{11} = \left(\frac{\rho B^4}{I_1}\right)C_{12} = \left(\frac{\rho B^4}{I_1}\right)C_{22} = 0.277$$

$$\left(\frac{\rho B^2}{M_1}\right)C_{11} = \left(\frac{\rho B^2}{M_1}\right)C_{12} = \left(\frac{\rho B^2}{M_1}\right)C_{22} = 0.0334$$

It will be assumed that $\omega_\alpha = 2 \omega_h$ and that $\omega_h = 2\pi(.1 \text{ Hz})$.

U/NB	A_1^*	A_2^*	A_3^*	H_1^*	H_2^*	H_3^*
2	0	0	0	-0.67	0	0
4	0	-0.03	0	-1.50	0	-0.05
6	0.75	-0.05	0.50	-2.05	0.7	-1.25
8	0.70	-0.10	1.00	-3.25	2.25	-3.35
10	0.68	-0.14	1.46	-4.25	4.25	-4.00
12	0.70	-0.16	1.69	-5.50	8.90	-5.00

CUBIC EQUATION

$$b_0 = 2(.01)(2)^2 + 2(.01)^2 = 0.12$$

$$b_1 = -0.1336 H_1^* - 0.277 A_2^*$$

$$b_2 = -0.06 - 0.00554 A_3^*$$

$$b_3 = 0.0277 A_2^* + 0.0334 H_1^* + .00925 [H_1^* A_3^* - A_1^* H_3^*]$$

U/NB = 12 (K = .523)

$$b_0 = .12$$

$$b_1 = (-.1336)(-5.50) - 0.277(-.16) = .7791$$

$$b_2 = -.06 - 0.00554(1.69) = -.06936$$

$$b_3 = (.277)(-.16) + [.0334)(-5.5) \\ + .00925 [(-5.5)(1.69) + 5(.70)] \\ = -.2816$$

$$(-.2816)x^3 - (.06936)x^2 + (.7791)x + .12 = 0$$

$$x^3 + (.2462)x^2 - 2.7667x - .4261 = 0$$

$$x = 1.62$$

(Negative roots neglected)

$$\underline{U/NB = 10} \quad (K = .628)$$

$$b_0 = .12$$

$$b_1 = (-.1336)(-4.25) - (.277)(-.14) = 0.6066$$

$$b_2 = -.06 - .00554(1.46) = -.06809$$

$$\begin{aligned} b_3 &= (.277)(-.14) + .0334(-4.25) \\ &\quad + .00925 [(-4.25)(1.46) + 4(.68)] \\ &= -.2130 \end{aligned}$$

$$(-.2130)x^3 - (.06809)x^2 + (.6066)x + .12 = 0$$

$$x^3 + .3197 x^2 - 2.848 x - .5634 = 0$$

$$x = 1.63$$

$$\underline{U/NB = 8} \quad (K = .785)$$

$$b_0 = .12$$

$$b_1 = (-.1336)(-3.25) - .277(-.10) = 0.4619$$

$$b_2 = -.06 - (.00554)(1.00) = -.06554$$

$$\begin{aligned} b_3 &= (.277)(-.10) + (.0334)(-3.25) \\ &\quad + .00925 [(-3.25) + 3.35(.70)] \\ &= -.1446 \end{aligned}$$

$$(-.1446)x^3 - (.06554)x^2 + .4619 x + .12 = 0$$

$$x^3 + (.4533)x^2 - (3.194)x - .8299 = 0$$

$$x = 1.71$$

$$\underline{U/NB} = 6 \quad (K = 1.05)$$

$$b_0 = .12$$

$$b_1 = (-.1336)(-2.05) - (.277)(-.05) = .2877$$

$$b_2 = -.06 - (.00554)(0.50) = -.06277$$

$$\begin{aligned} b_3 &= (.277)(-.05) + (.0334)(-2.05) \\ &\quad + .00925 [(-2.05)(.50) - (.75)(-1.25)] \\ &= -0.0831 \end{aligned}$$

$$(-.0831)x^3 - (.06277)x^2 + (.2877)x + .12 = 0$$

$$x^3 + (.7554)x^2 - 3.462x - 1.444 = 0$$

$$x = 1.73$$

$$\underline{U/NB} = 4 \quad (K = 1.57)$$

$$b_0 = .12$$

$$b_1 = (-.1336)(-1.50) - .277(-.03) = .2087$$

$$b_2 = -.06 - .0054(0) = -.06$$

$$b_3 = -.00831 + .0334(-1.5) = -.0584$$

$$(-.0584)x^3 - (.06)x^2 + (.2087)x + .12 = 0$$

$$x^3 + (1.027)x^2 - (3.574)x - 2.055 = 0$$

$$x = 1.73$$

$$\underline{U/NB} = 2 \quad (K = 3.14)$$

$$b_0 = .12$$

$$b_1 = (-.1336)(-0.67) - (.277)(0) = .08951$$

$$b_2 = -.06$$

$$b_3 = (.0334)(-.67) = -.02238$$

$$(-.02238)x^3 - (.06)x^2 + (.08951)x + .12 = 0$$

$$x^3 + 2.681x^2 - 4.00x - 5.362 = 0$$

$$x = 1.63$$

Quartic Equation

$$a_0 = (2)^2 = 4$$

$$a_1 = 0$$

$$a_2 = -5.0008 - .277 A_3^*$$

$$a_3 = .00134 H_1^* + .00554 A_2^*$$

$$a_4 = 1 + .277 A_3^* + .00953 [A_1^* H_2^* - A_2^* H_1^*]$$

$$\underline{U/NB} = 12 \quad (K = .523)$$

$$a_0 = 4$$

$$a_1 = 0$$

$$a_2 = -5.0008 - (2.77)(1.69) = -5.469$$

$$a_3 = (.00134)(-5.50) + (.00554)(-.16) = -.00826 \text{ (neglig.)}$$

$$a_4 = 1 + (.277)(1.69) + .00953 [(.70)(8.9) - 5.50(.16)]$$

$$= 1.519$$

$$(1.519)x^4 - 5.469x^2 + 4 = 0$$

$$x^2 = \frac{5.469 \pm \sqrt{(5.469)^2 - 4(4)(1.519)}}{2(1.519)}$$

$$x^2 = 2.579, \quad 1.021$$

$$x = 1.61, \quad 1.01$$

$$\underline{U/NB = 10} \quad (K = .628)$$

$$a_0 = 4$$

$$a_1 = 0$$

$$a_2 = -5.0008 - (.277)(1.46) = -5.405$$

$$a_3 = \text{negligible}$$

$$a_4 = 1 + (.277)(1.46) + .00953 [(.68)(4.25) - (4.25)(.14)]$$

$$= 1.426$$

$$1.426 x^4 - 5.405 x^2 + 4 = 0$$

$$x^2 = \frac{5.405 \pm \sqrt{(5.405)^2 - 4(4)(1.426)}}{2(1.426)}$$

$$x^2 = 2.782, \quad 1.008$$

$$x = 1.67, \quad 1.00$$

$$\underline{U/NB} = 8 \quad (K = .785)$$

$$a_0 = 4$$

$$a_1 = 0$$

$$a_2 = -5.0008 - (.277)(1.00) = -5.278$$

$$a_3 = \text{negligible}$$

$$a_4 = 1 + (.277)(1.00) + .00953 [(.70)(2.25) - (.10)(3.25)] \\ = 1.289$$

$$1.289 X^4 - 5.278 X^2 + 4 = 0$$

$$X^2 = \frac{5.278 \pm \sqrt{(5.278)^2 - 4(4)(1.289)}}{2(1.289)}$$

$$X^2 = 3.091 \quad , \quad 1.004$$

$$X = 1.76 \quad , \quad 1.00$$

$$\underline{U/NB} = 6 \quad (K = 1.05)$$

$$a_0 = 4$$

$$a_1 = 0$$

$$a_2 = -5.0008 - .277(.50) = -5.139$$

$$a_3 = \text{negligible}$$

$$a_4 = 1 + (.277)(.50) + .00953 [(.75)(.70) - 2.05 (.05)] \\ = 1.143$$

$$(1.143) x^4 - 5.139 x^2 + 4 = 0$$

$$x^2 = \frac{5.139 \pm \sqrt{(5.139)^2 - 4(4)(1.143)}}{2(1.143)}$$

$$x^2 = 3.495, 1.001$$

$$x = 1.87, 1.00$$

$$\underline{U/NB = 4} \quad (K = 1.57)$$

$$a_0 = 4$$

$$a_1 = 0$$

$$a_2 = -5.0008$$

$$a_3 = \text{negligible}$$

$$a_4 = 1.000$$

$$x^2 = \frac{5.0008 \pm \sqrt{(5.0008)^2 - 16}}{2}$$

$$x^2 = 4.001, .99973$$

$$x = 2.000, 1.000$$

$$\underline{U/NB = 2.0} \quad (K = 3.14)$$

$$a_0 = 4$$

$$a_1 = 0$$

$$a_2 = -5.0008$$

$$a_4 = 1.00$$

$$x = 2.000, 1.000$$

$$\text{VALUES OF } X = \frac{\omega}{\omega h}$$

<u>U/NB</u>	<u>K</u>	<u>Cubic Eq.</u>	<u>Quartic Eq.</u>	
2	3.14	1.66	1.00	2.00
4	1.57	1.73	1.00	2.00
6	1.05	1.73	1.00	1.87
8	.785	1.71	1.00	1.76
10	.628	1.63	1.00	1.67
12	.523	1.62	1.01	1.61

Cubic equation intersects quartic equation at

$$X = 1.62 \quad K = .53 \quad (U/NB = 11.7)$$

Therefore,

$$U_c = \frac{B \omega h X_c}{K_c}$$

$$U_c = \frac{(100 \text{ ft}) [2\pi (.1)] 1.62}{0.53}$$

$$U_c = 190.3 \text{ ft/sec} = 129.7 \text{ mph}$$

REFERENCES FOR SECTION III

- [3.1] Scanlan, R.H.: "Recent Methods in the Application of Test Results to the Wind Design of Long, Suspended-Span Bridges," Report No. FHWA-RD-75-115, Federal Highway Administration Office of Research and Development, Washington, DC, 1975.
- [3.2] Simiu, E. and Scanlan, R.H.: Wind Effects on Structures, Wiley, New York, 1978.
- [3.3] Scanlan, R.H. and Tomko, J.J.: "Airfoil and Bridge Deck Flutter Derivatives," Jnl. Eng. Mech. Div. ASCE, Vol. 97, No. EM6, Dec. 1971, pp. 1717-1737.

IV. A VORTEX SHEDDING MODEL IN THE BRIDGE CONTEXT

Introduction

Many complex analytical models of the vortex-shedding phenomenon have been published in the literature. Ref. [4.1]^{*} cites a considerable number of these. All of the models are empirical in nature and depend upon experiment for the evaluation of the several constants that occur in them. The number of constants is greater if the details of physical response sought to be represented are fine-grained, or very accurate.

The phenomenon of vortex shedding, and the "lock-in" (or "lock-on") phenomenon associated with it in the case of flexible structures are well known in their general characteristics. However, a few salient features will be reviewed here as a setting for the ideas to be presented below.

When wind blows across an elongated, bluff object, the wake of the object often shows a coherent set of alternating vortices discharged downwind. These vortices are initiated, in detail, by the fine physical constitution of the fluid flow as it is variously sheared by the effects of body cross-sectional shape. The mechanism, very broadly speaking, can be described as an interaction between the inertial and viscous forces of the fluid as they are influenced by body geometry. Hence the flow regimes in which vortex shedding is manifest are a function of Reynolds number.

For a wide range of Reynolds number of interest to engineering, however, the rhythm of alternate vortex shedding is governed by the simple Strouhal relation

$$\frac{n_s A}{U} = S \quad ,$$

^{*} Numbers in brackets refer to listing at the end of Section IV.

where n_s is the frequency of complete cycles of vortex shedding, U is the cross-flow velocity of the fluid, A is the across-flow projected area of the body per unit of its span, and S is the Strouhal number, nearly a constant, dependent mainly on body geometric shape. For a circular cross-section, for example, $S \approx 0.2$. The Strouhal number for various bluff bodies typically ranges between 0.1 and 0.3. For a given new bridge deck cross-section, it must, however, be determined from experiment. Table 4.1 [4.2] lists some Strouhal numbers for specified directions of fluid flow for some typical structural forms.

If the bluff body is elastically supported, the alternating fluid pressures on it that accompany the vortex shedding phenomenon will cause it to deflect alternately, either across the flow, or in twist. This deflection, for engineering structures, may be considered to be unimportant except in those cases when the Strouhal vortex shedding rhythm approaches closely to a natural frequency of the structure. In such cases, the structure may "resonate" and so deflect appreciably, and in so doing, its motion also affects the local boundary conditions influencing the fluid action. What is observed overall in such cases, is the following aeroelastic phenomenon.

The vortex-shedding frequency is directly proportional to wind velocity; when this velocity is such as to elicit a natural structural frequency by the proper vortex-shedding rhythm, the resulting structural motion causes the vortex shedding phenomenon to "lock on" to the rhythm established by the structure. This condition prevails over a range of wind velocities exceeding the initial lock-on value. Appreciably higher wind velocity is then required before a vortex rhythm sufficiently "out of tune" with the structural rhythm occurs so as to break up the "lock-in" phenomenon and lower the strength of the response.

	S 0.14 0.12		S 0.15
	0.14 0.18		0.15
	0.15		0.14 0.15
	0.18 0.16		0.15
	0.15 0.14 0.18		0.12
	0.17 0.15		0.14
	0.17 0.18		0.16
	0.18 0.18		0.15
	0.15 0.16		0.20

TABLE 4.1 [4.2]

Strouhal Number S Based on d for Typical Structural Sections

Fig. 4.1 depicts the trend of the lock-on phenomenon.

It has in fact, been demonstrated by certain careful experiments [4.3], that the spectrum of across-wind force acting on the bluff body always contains at least the two important components -- one at the Strouhal-governed frequency, and the other at the structure-governed frequency. The relative magnitudes of these components vary as the velocity and structural motion vary. However, when the two frequencies are close together, lock-on of vortex shedding has its greatest effect, giving rise to greatest structural oscillation amplitude.

Researchers have sought empirical mathematical models that reflect the main phenomenological points qualitatively described above. Such models have, in general, had no difficulty in representing gross structural behavior-- which is reasonably modeled as that of a simple linear, elastic oscillator; but numerous difficulties have been encountered with the range of fluid oscillator properties and overall performance characteristics. The most common tendency then in the analytical models to be found in the literature is to provide for a quasi-independent "fluid oscillator" that is coupled in some manner to the structural oscillator.

Since all models described to date in the literature are heavily empirical, the particular model selected for a given purpose can scarcely support claims to a deep underlying physical insight; rather it represents, at its most favorable, the simplest device intended to accomplish a given end, namely, the forecasting of the sought-after character of a new event based on observations of similar past events.

In bridge wind engineering, the vortex shedding phenomenon presents itself in the following situations. A long-span, flexible bridge may, at a relatively low cross-wind velocity, exhibit oscillations of limited

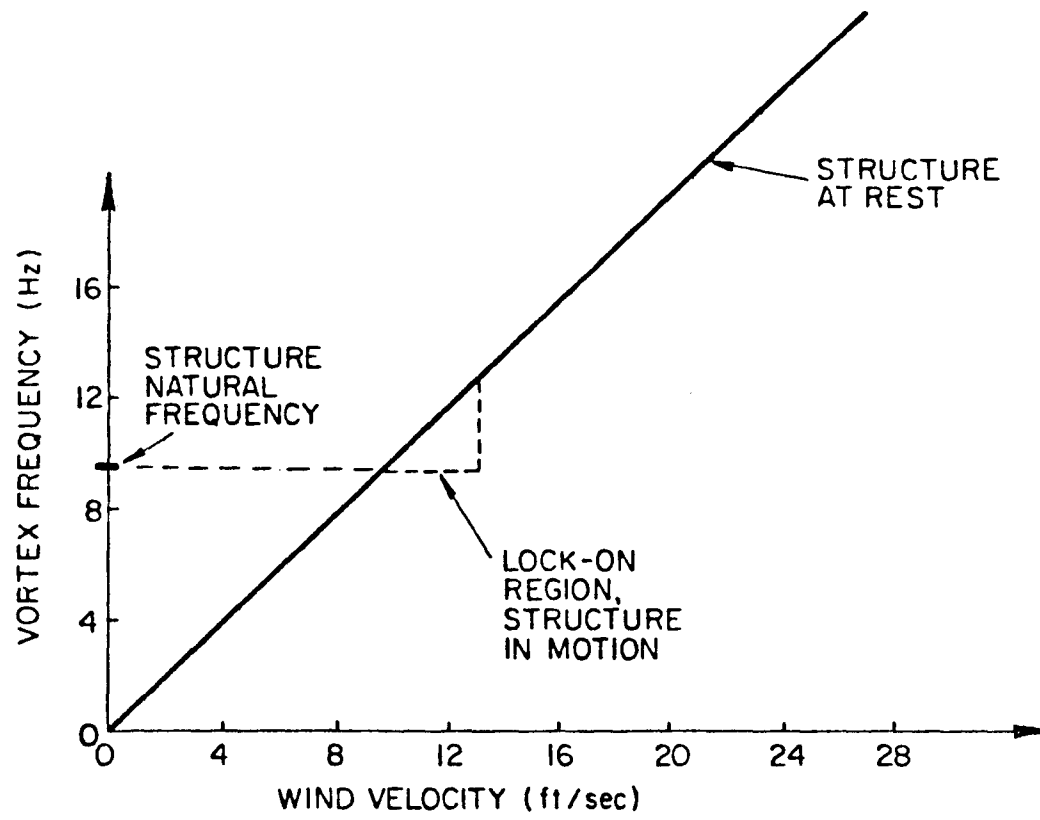


FIGURE 4.1

FREQUENCY CHARACTERISTICS OF VORTEX SHEDDING

amplitude that can be fatiguing to the structure or annoying to its users. When a section model of the same bridge, with geometrically similar deck, is mounted elastically in a wind tunnel, the same vortex shedding and lock-on phenomena are exhibited at some scaled velocity.

The problem confronting the wind engineer then simply is to predict, from observation of the scaled section model, the maximum amplitudes to be expected in the prototype. It will be noted that, in this circumstance, not all aspects of the complex phenomenon of vortex shedding need be reproduced by an analytical model. All that is required is that, given observation of a scaled section model at locked-in "resonance", the corresponding "worst case" of the prototype be forecast for design purposes.

This circumstance implies only that whatever analytical model is used be capable of transcribing the observed wind tunnel model behavior at "resonance" over to prototype behavior, and that prior and post states of excitation need not be of concern.

What is in fact observed in the wind tunnel is that, at lock-in wind speed, a model released in the cross-wind will oscillate in a self-excited manner, with growing amplitude, until a maximum limiting amplitude is achieved and thereafter maintained as a steady-state oscillation. This limiting amplitude is a function of the mechanical damping of the model and, of course, is also highly dependent upon the model geometric shape.

In the context then of these circumstances, a simple, self-limiting, nonlinear oscillator of the Van der Pol type will be suggested as a forecasting model in the present report. Means will be described for determining its two aerodynamic parameters, and an extrapolation from bridge section model to prototype full-span bridge will be outlined.

4.1 Analytical Model of the Deck Section (Vertical Motion)

The analytics of response to vortex shedding will first be discussed with attention to the more pronounced response direction--vertical. In Section 4.6, some remarks on torsional response will be made.

Consider a deck section model, of deck width B, projected (windward) area per unit span A, vertical deflection coordinate h, and mass per unit span m. The following nonlinear analytical model of its vertical vortex-induced motion is proposed:

$$(4.1) \quad m[\ddot{h} + 2\xi_h\omega_h\dot{h} + \omega_h^2h] = \frac{1}{2} \rho U^2(2B)H_0^*(1 - \epsilon^2 \frac{h^2}{B^2}) \frac{\dot{h}}{U}$$

where

- ξ_h = damping ratio in h-motion
- ω_h = natural circular frequency in h-motion
- ρ = air density
- H_0^* = aerodynamic damping coefficient
- ϵ^2 = nonlinear aerodynamic response coefficient
- U = steady cross-wind velocity.

The model proposed is nonlinear, but, based on some laboratory observation, the response will nonetheless be assumed to take, approximately, the same form as that of a linear oscillator:

$$(4.2) \quad h = h_0 \cos \omega t$$

where present interest will be focussed only on the case

$$(4.3) \quad \omega \approx \omega_h$$

and

$$(4.4) \quad \frac{\omega A}{U} = 2\pi S$$

where S is the Strouhal number governing vortex shedding for the deck cross-section.

The vertical velocity of deck motion is

$$(4.5) \quad \dot{h} = -\omega h_0 \sin \omega t$$

The total damping force per unit span is then

$$(4.6) \quad F_d = \left[2 m \xi_h \omega h - \rho U B H_0^* \left(1 - \epsilon^2 \frac{h^2}{B^2} \right) \right] \dot{h}$$

This will vary in time, according to (4.2), as h varies.

The average damping energy per cycle (energy lost, plus energy gained), will be zero if conditions are such that a steady oscillation is maintained.

This is calculated by the integral

$$(4.7) \quad \int_0^T F_d \dot{h} dt = 0$$

where $\omega T = 2\pi$.

Thus (4.7) is equivalent to

$$(4.8) \quad \left[2 m \xi_h \omega h - \rho U B H_0^* \right] \int_0^T \dot{h}^2 dt + \frac{\rho U B H_0^* \epsilon^2}{B^2} \int_0^T h^2 \dot{h}^2 dt = 0$$

But

$$(4.9) \quad \int_0^{2\pi/\omega} (-\omega h_0 \sin \omega t)^2 dt = \pi \omega h_0^2$$

$$(4.10) \quad \int_0^{2\pi/\omega} (h_0 \cos \omega t)^2 (-\omega h_0 \sin \omega t)^2 dt = \frac{\pi}{4} \omega h_0^4 ,$$

whence (4.8), with use of (4.3 and 4.4), leads to the following expression for h_0 :

$$(4.11) \quad h_0 = \frac{2B}{\varepsilon} \left[1 - \frac{4 \pi m \zeta_n S}{\rho AB H_0^*} \right]^{1/2}$$

This expresses the oscillation amplitude as a function of mechanical parameters and the two aerodynamic parameters ε and H_0^* , which must be determined from experiment.

It will be noted that the dimensionless term, $R \zeta_h / H_0^*$ with R defined as

$$(4.12) \quad R = \frac{4 \pi m S}{\rho AB}$$

combines the physical characteristics of the system: ratio of structure to air masses; ratio of mechanical to aerodynamic damping; and Strouhal number characteristic of structure geometry. It should also be remarked that the case $\varepsilon \rightarrow 0$ (no nonlinear damping term), does in fact, correspond to a "critical instability" case of zero damping, when $2m \zeta_h \omega_h = \rho UB H_0^*$. However, this case is here ruled out physically by observation of only finite-amplitude vortex-induced oscillations in laboratory experiments. [See, however, the differing case of torsional *flutter*, Section III].

4.2 Evaluation of Constants in the Analytical Model

Eq. 4.11 contains two unknown constants, ε and H_0^* , that must be evaluated by experiment. As stated earlier, the mechanical damping influences

the response amplitude. Hence a pair of response experiments, each with a different mechanical damping, suffices to establish values of ϵ and H_0^* for this model. Let (h_{o1}, ζ_{h1}) and (h_{o2}, ζ_{h2}) be the pairs of amplitude and corresponding mechanical damping ratios used in two successive deck model "resonance" experiments at the lock-in Strouhal frequency. Then, from (4.11) and (4.12):

$$(4.13) \quad H_0^* = \frac{R[\zeta_{h1} - \frac{h_{o1}^2}{h_{o2}^2} \zeta_{h2}]}{1 - h_{o1}^2/h_{o2}^2}$$

and from (4.11),

$$(4.14) \quad \epsilon^2 = \frac{4B^2}{h_o^2} \left[1 - R \frac{\zeta_h}{H_o^*} \right]$$

where the value of h_o used is either h_{o1} or h_{o2} , with ζ_h corresponding, and H_o^* comes from (4.13).

4.3 Analytical Model of the Full Bridge

Since the phenomenon of vortex lock-in "selects" a particular mode for "resonance", this condition will be modeled; that is, it will be assumed that a Van der Pol type oscillator response at the natural frequency of a given mode is taking place, excited by aerodynamic forces with wind at appropriate velocity. In this model, complete coherence of all aerodynamic forces along the bridge span will be assumed. This assumption is conservative, as discussed in Ref. [4.1], but at lock-in, the coherence of

aerodynamic effects along the span is much greater than in its absence. It is expected that the model can therefore, with proper experimental input, furnish a preliminary conservative criterion for use in design. Adjustment for spanwise loss of coherence will be considered at a later point.

Eqn. 4.1 above holds for any spanwise deck section. Letting x be the spanwise deck coordinate, the vertical motion h at x can be expressed as

$$(4.15) \quad h(x,t) = \phi(x) \xi(t) B$$

where $\phi(x)$ is the spanwise shape of the mode involved, $\xi(t)$ is its generalized coordinate, both nondimensional; the factor B is included for dimensional compatibility with that of deflection h .

The definition (4.15) may be inserted into (4.1), the result multiplied by $\phi(x)$, and integrated over the span length L of the deck. This yields

$$(4.16) \quad M[\ddot{\xi} + 2 \zeta_h \omega_h \dot{\xi}_h + \omega_h^2 \xi] = \rho UBL H_0^* [\phi_2 - \epsilon^2 \phi_4 \xi^2] \dot{\xi}$$

where

$$(4.17) \quad M = \int_0^L m \phi^2 dx \quad (\text{generalized mass})$$

$$(4.18) \quad \phi_2 = \int_0^L \phi^2 \frac{dx}{L}$$

$$(4.19) \quad \phi_4 = \int_0^L \phi^4 \frac{dx}{L} .$$

The criterion that the net energy loss per cycle is zero may now be applied, i.e., for $\omega T = 2\pi$:

$$(4.20) \quad \int_0^T [2 M \zeta_h \omega_h - \rho UBL H_0^* (\Phi_2 - \epsilon^2 \Phi_4 \xi^2)] \dot{\xi}^2 dt = 0$$

which, for an assumed approximate response form of

$$\xi = \xi_0 \cos \omega t$$

yields the criterion

$$(4.21) \quad [2 M \zeta_h \omega_h - \rho UBL H_0^* \Phi_2] \pi \omega \xi_0^2 + \rho UBL H_0^* \epsilon^2 \Phi_4 \frac{\pi}{4} \omega \xi_0^4 = 0 .$$

This yields, for the response amplitude ξ_0 of the generalized coordinate:

$$(4.22) \quad \xi_0 = \frac{2}{\epsilon} \left[\frac{\Phi_2 - \frac{4 \pi M \zeta_h S}{\rho ABL \Phi_4 H_0^*}}{\Phi_4} \right]^{\frac{1}{2}}$$

where, as noted earlier, S is the Strouhal number for the section and A is its projected (frontal) cross-wind area per unit span; the aerodynamic parameters ϵ and H_0^* are as determined from experiment in the preceding section.

The spanwise distribution of maximum displacement is then given, from (4.15), as:

$$(4.23) \quad h(x) = B \xi_0 \phi(x)$$

4.4 Example

Consider a bridge span $L = 600$ ft (183 m) with a running weight per foot of span of 4,500 lb. (6709 kg/m). Assume a Strouhal number of $S = 0.15$ at a frequency of $n = 0.5$ Hz, with a corresponding bridge vertical mode that is a half sine wave over the span. Assume a deck width $B = 30$ ft (9.15 m) and a frontal area per unit span of $A = 5$ ft. (1.52 m).

Assume that a 1/30-scale section model, 5 ft (1.52 m) long, of this bridge has been tested at vortex-shedding lock-in with the following results:

<u>Damping Ratio</u> ζ	<u>Amplitude</u> h_0
0.005	0.25 inch (0.64 cm)
0.035	0.125 inch (0.32 cm)

From (4.12) (either for model or prototype, assuming the model correctly scaled):

$$R = \frac{4\pi m S}{\rho AB} = \frac{4\pi \cdot \frac{4500}{32.2} \cdot 0.15}{0.002378 \cdot 5 \cdot 30} = 738.5$$

From (4.13):

$$H_0^* = \frac{738.5[0.005 - 4(0.035)]}{1 - 4} = 33.233$$

From (4.14) (using model data)

$$\epsilon^2 = \frac{4 \times 12^2}{(0.25)^2} \left[1 - 738.5 \frac{0.005}{33.233} \right] = 8192$$

so that

$$\epsilon = 90.51$$

For $\frac{1}{2}$ sine waves, $\phi_2 = \frac{1}{2}$ and $\phi_4 = \frac{3}{8}$. Then, from (4.22), for the assumed value $\zeta_h = 0.01$:

$$\xi_0 = \frac{2}{90.51} \left[\frac{0.5}{0.375} - 738.5 \left(\frac{0.5}{0.375} \right) \frac{0.01}{33.233} \right]^{\frac{1}{2}} = 0.0225$$

From (4.23), the maximum deflection amplitude $h(x)$ (at center span, $x = L/2$) is then

$$h(x) = 30 \times 0.0225 = 0.675 \text{ ft. (0.206 m)}$$

The double amplitude (total excursion) will be 1.35 ft. (0.411 m). Note that the prototype, full bridge maximum amplitude does not scale simply as the scale factor (30) times the observed single amplitude ($\sim \frac{1}{4}$ in.) of the section model. The average full bridge amplitude is $\frac{2}{\pi} \times 0.675 = 0.43 \text{ ft. (0.131 m)}$. In the present example to this point, 100% correlation of spanwise effects has been assumed.

4.5 Correction for Loss of Spanwise Coherence

Spanwise coherence of force effects falls off rapidly in turbulent flow conditions, (cf. [4.5] and Section V), but the phenomenon of lock-on acts as a controller and coordinator of such effects, lessening considerably the rate of aerodynamic force fall-off with distance along the span from a given reference point. Not a large quantity of data are available to

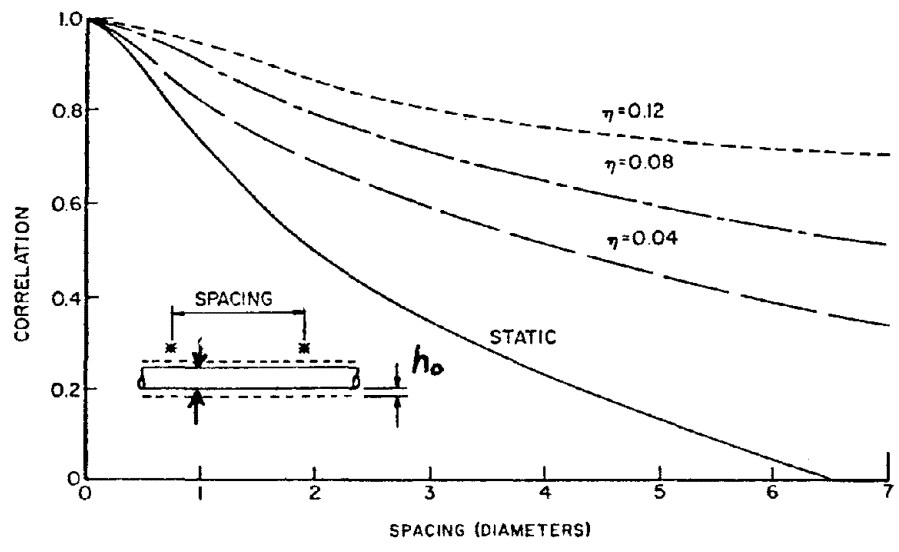


FIGURE 4.2 [4.1]

Correlation of Vortex Shedding from Circular Cylinder at Lock-in

document this point, but Fig. 4.2, drawn from Refs. [4.1], [4.4], [4.5], presents some information on the effect of vortex lock-on spanwise correlation in the case of a circular cylinder oscillated at various amplitudes $\eta = h_0/A$.

The phenomenon of the spanwise coherence of lock-on vortex induced forces requires further research, particularly experimental. It is clear, however, from Fig. 4.2 that some loss of coherence must be accounted for, both for the reason of natural turbulent loss at constant oscillation amplitude and the reason of decreasing deflection of the mode away from its highest point.

As a simple qualitative approach to these two effects, it will first be assumed here that the only portion of the deck that is effective in producing lock-on forces is the central half near the peak of the mode. Under these conditions, the driving vortex forces in the example cited above should be modified by integrating them only from $L/4$ to $\frac{3L}{4}$ instead of completely across the span, 0 to L .

With this modification, Φ_2 and Φ_4 are changed to:

$$\Phi_2^m = \int_{L/4}^{3L/4} \sin^2 \frac{\pi x}{L} \frac{dx}{L} = 0.40915$$

and

$$\Phi_4^m = \int_{L/4}^{3L/4} \sin^4 \frac{\pi x}{L} \frac{dx}{L} = 0.34665$$

Thus ξ_0 is calculated from the modified formula

$$\xi_0 = \frac{2}{\epsilon} \left[\frac{\Phi_2^m}{\Phi_4^m} - R \frac{\Phi_2 \zeta_n}{\Phi_4 H_0} \right]$$

This yields

$$\begin{aligned}\xi_0 &= \frac{2}{90.51} \left[\frac{0.40915}{0.34665} - 738.5 \frac{0.5 \times 0.01}{0.34665 \times 33.233} \right]^{1/2} \\ &= 0.02049\end{aligned}$$

which yields a maximum single amplitude of

$$h_0 = 30 \times 0.02049 = 0.615 \text{ ft. (0.188 m)}$$

It will be observed that the relatively strong assumption -- that only the central half of the mode participates in the locked-on vortex driving -- does not result in an impressive reduction of the response amplitude, reducing it by only about 9%.

Using this same approach with an even stronger assumption, namely that only the central third of the span contributes to the vortex driving force, results in the values

$$\begin{aligned}\phi_2^m &= \int_{L/3}^{2L/3} \sin^2 \frac{\pi x}{L} \frac{dx}{L} = 0.30450 \\ \phi_4^m &= \int_{L/3}^{2L/3} \sin^4 \frac{\pi x}{L} \frac{dx}{L} = 0.29730\end{aligned}$$

with the result for ξ_0 :

$$\begin{aligned} \xi_0 &= \frac{2}{90.51} \left[\frac{0.30450}{0.29730} - 738.5 \frac{0.5 \times 0.01}{0.29730 \times 33.233} \right]^{1/2} \\ &= 0.01782 \end{aligned}$$

with the consequent value for h_0 :

$$h_0 = 30 \times 0.01782 = 0.535 \text{ ft. (0.164 m)}$$

which represents about a 20% reduction in amplitude from the case of assumed complete span correlation of vortex forces.

It may be tentatively concluded that calculations based on complete spanwise correlation of vortex effects constitute a conservative upper bound to the expected prototype vortex-induced deflections.

The entire area of vortex-induced oscillation is still in need of further research, particularly at the experimental level. The methodology presently offered can, however, serve to bound expected prototype responses when wind tunnel model data are available as a sound basis for calculation.

Overall, the loss of spanwise coherence among aerodynamic forces in the case of vortex lock-in is not expected to be as strong as that which occurs under random turbulence. The present correction factors are, of course, purely empirical and are based on the small amount of evidence presently available from circular cylinders. The coherence question is clearly in need of further research of an experimental nature, pointed particularly at the bluff-body problem presented by typical bridge deck forms.

4.6 Remarks on Torsional Response

The equation of sectional motion in the torsional case is

$$(4.24) \quad I[\ddot{\alpha} + 2 \zeta_{\alpha} \omega_{\alpha} \dot{\alpha} + \omega_{\alpha}^2 \alpha] = \frac{1}{2} \rho U^2 (2B^2) A_0^* (1 - e^2 \alpha^2) \frac{B \dot{\alpha}}{U}$$

where the notation is as in the flutter case, with the additions:

A_0^* = aerodynamic damping coefficient

e^2 = nonlinear aerodynamic response coefficient.

The motion at "resonance" may be assumed as approximately of the form

$$(4.25) \quad \alpha = \alpha_0 \cos \omega t$$

where

$$(4.26) \quad \omega \approx \omega_{\alpha}$$

and

$$(4.27) \quad \frac{\omega A}{U} = 2\pi S$$

The analogous result to (4.11) for amplitude α_0 becomes

$$(4.28) \quad \alpha_0 = \frac{2}{e} \left[1 - \frac{Q \zeta_{\alpha}}{A_0^*} \right]^{\frac{1}{2}}$$

where the dimensionless ratio Q is defined as

$$(4.29) \quad Q = \frac{4\pi I}{\rho A B^3} S$$

The defining equations for A_0^* and e^2 are then

$$(4.30) \quad A_0^* = \frac{Q[\zeta_{\alpha 1} - (\frac{\alpha_{01}}{\alpha_{02}})^2 \zeta_{\alpha 2}]}{1 - (\alpha_{01}/\alpha_{02})^2}$$

$$(4.31) \quad e^2 = \frac{4}{\alpha_0^2} \left[1 - Q \frac{\zeta_{\alpha}}{A_0^*} \right]$$

for experimentally observed amplitudes α_{01} , α_{02} associated with mechanical damping values $\zeta_{\alpha 1}$, $\zeta_{\alpha 2}$, respectively.

Defining now the torsional response in the first mode $\psi(x)$ to be

$$(4.32) \quad \alpha(x,t) = \psi(x) \eta(t)$$

where $\psi(t)$ is a generalized coordinate responding as

$$(4.33) \quad \eta = \eta_0 \cos \omega t$$

leads to the following result for α_0 :

$$(4.34) \quad \eta_0 = \frac{2}{e} \left[\frac{\psi_2}{\psi_4} - \frac{4\pi I_0 \zeta_{\alpha} S}{\rho AB^3 L \psi_4 A_0^*} \right]^{\frac{1}{2}}$$

where

$$(4.35) \quad \psi_2 = \int_0^L \psi^2(x) \frac{dx}{L}$$

$$(4.36) \quad \psi_4 = \int_0^L \psi^4(x) \frac{dx}{L}$$

$$(4.37) \quad I_0 = \int_0^L I(x) \psi^2(x) dx \quad (\text{generalized moment of inertia})$$

The distributed maximum torsional displacement is then

$$(4.38) \quad \alpha(x) = \eta_0 \psi(x) .$$

The problem is treated in all respects as analogous to the vertical response problem. Interest in either problem depends, of course, upon direct evidence of vortex excitation witnessed on a wind tunnel model of the bridge deck section in question.

REFERENCES FOR SECTION IV

- [4.1] Simiu, E. and Scanlan, R.H.: Wind Effects on Structures, Wiley, N.Y., 1978.
- [4.2] Jensen, M.: Aerodynamik i den Naturlige Vind, Teknisk Forlag, København, 1959.
- [4.3] Otsuki, Y., Washizu, K. and A. Ohya: "Wind Tunnel Experiments on the Aeroelastic Instability of a Prismatic Model with a Rectangular Section," 75-AM, JSME A-15, Proceedings Joint Japan and American Societies of Mechanical Engineers Applied Mechanics Western Conf., Honolulu, Hawaii, March 1975, pp. 145-152.
- [4.4] Wooton, L.R. and C. Scruton: "Aerodynamic Stability," in The Modern Design of Wind-Sensitive Structures, Construction Industry Research and Information Association, London, 1971.
- [4.5] Toebes, G.H.: "Fluidelastic Features of Flow Around Cylinders," Proc. Int'l. Research Seminar on Wind Effects on Bldgs. and Structures, Ottawa, Canada, 1967, Vol. 2, Univ. of Toronto Press, Toronto, 1968, pp. 323-334.

V. PARAMETERS AFFECTING LONG-SPAN BRIDGE BUFFETING SUSCEPTIBILITY

Introduction

Since 1960 there have appeared a number of publications (see Refs. [5.1]-[5.22], at the end of this section) dealing with both theory and test relative to the buffeting of suspended-span bridges by natural turbulent wind. The present section returns to Ref. [5.18] and reexamines the theory relative to the buffeting, first of single torsional modes, and second, of single vertical modes.

Torsional modes are, in one sense, more interesting than vertical ones because of the not infrequent occurrence of effectively negative aerodynamic damping associated with these modes, especially in older bridges where this tendency was not specifically avoided by design characteristics initially. Such tendencies are associated with a prominent variety of bridge flutter.

The theory of Ref. [5.18] culminates in a pair of formulas for maximum mean-square buffeting deflections beyond the mean steady deflections, as distributed along the bridge span. These formulas are first reexamined, some additional effects are included in them, and a representative parameter study is then made. In particular, the role of each parameter is emphasized, together with the trend of the dependence of buffeting deflections upon it.

After an examination of theoretical implications in each case: torsion and bending, a set of six successive hypothetical modes is postulated for the main span of a long bridge. Using arbitrary but representative parameters, the average response of each of the modes is calculated in turn. The study permits an evaluation of trends. No intermodal coupling, aerodynamic or otherwise, is considered in the present study. While this is possibly

important in certain few cases, it is not considered important enough to require inclusion in all routine calculations of buffeting response.

The study will be of interest to designers and retrofitters of older bridges as well as to those interested in the interpretation of wind tunnel model results on long-span bridges.

5.1 Theory for Torsion

Let α be the torsional degree of freedom of the bridge deck, with $\alpha(x,t)$ denoting a value of α varying in time at spanwise section x of a long-span bridge, such as a suspension bridge. If I is the mass moment of inertia of the bridge deck and its support cables per unit span about the local c.g. of the deck, then the section x twists according to the equation (cf. [5.18]):

$$(5.1) \quad I[\ddot{\alpha} + 2\zeta_{\alpha}\omega_{\alpha}\dot{\alpha} + \omega_{\alpha}^2\alpha] = \frac{1}{2} \rho \bar{U}^2 (2B^2) \\ \times [K A_1^* \frac{\dot{h}}{\bar{U}} + K A_2^* \frac{B\dot{\alpha}}{\bar{U}} + K^2 A_2 \alpha] + M_{\alpha}(x,t)$$

where

ζ_{α} = mechanical damping ratio in torsion

ω_{α} = natural circular frequency in torsion

ρ = air density

\bar{U} = mean wind velocity normal to the span

B = deck width

$K = \frac{B\omega}{\bar{U}}$ = "reduced frequency" of torsional motion

A_i^* ($i=1,2,3$) = bridge deck self-excited or "flutter" coefficient

(all A_i^* are functions of $\frac{\bar{U}}{nB} = \frac{2\pi}{K}$)

h = vertical motion of bridge c.g.

$M_\alpha(x,t)$ = aerodynamic buffeting moment per unit span on section x .

If the r^{th} single spanwise torsional mode $\alpha_r(x)$ is provisionally considered to be responding alone, or independently, let its response be designated by

$$(5.2) \quad \alpha(x,t) = \alpha_r(x)\eta_r(t)$$

where $\eta_r(t)$ is the associated generalized coordinate. Eq. 5.1 then generalizes, for this mode of the full bridge of span L , to

$$(5.3) \quad I_r[\ddot{\eta}_r(t) + 2\zeta_r\omega_r \dot{\eta}_r(t) + \omega_r^2\eta_r(t)] = \frac{1}{2}\rho\bar{U}^2(2B^2) K A_2^* G_r \frac{LB\dot{\eta}_r(t)}{\bar{U}} + \bar{M}_{\alpha,r}(t)$$

where self-excited aerodynamic terms in A_1^* and A_3^* have been dropped on the basis that their contribution is small or negligible (some experimental justification for this exists [5.17]), and

$$(5.4) \quad I_r = \int_0^L I \alpha_r^2(x) dx \quad (\text{the } r^{\text{th}} \text{ generalized inertia})$$

$$(5.5) \quad G_r = \int_0^L \alpha_r^2(x) dx/L \quad (\text{the } r^{\text{th}} \text{ modal factor})$$

$$(5.6) \quad \bar{M}_{\alpha,r}(t) = \int_0^L M_\alpha(x,t) \alpha_r(x) dx \quad (\text{generalized aerodynamic moment})$$

Defining a net damping ratio γ_r as

$$(5.7) \quad \gamma_r = \xi_r - \frac{\rho B^4 L}{2 I_r} A_2^* \left(\frac{\bar{U}}{n_r B} \right) G_r$$

where $A_2^* \left(\frac{\bar{U}}{n_r B} \right)$ is the value of A^* evaluated at $\frac{\bar{U}}{n_r B}$ for $n=n_r$, the torsional frequency of mode r in Hz, Eq. (5.3) becomes

$$(5.8) \quad I_r [\ddot{\eta}_r + 2\gamma_r \omega_r \dot{\eta}_r + \omega_r^2 \eta_r] = \int_0^L M_\alpha(x,t) \alpha_r(x) dx$$

The buffeting moment per unit span is

$$(5.9) \quad M_\alpha(x,t) = \frac{1}{2} \rho \bar{U}^2 B^2 \left[C_M \frac{2u(x,t)}{\bar{U}} + C_M' \frac{w(x,t)}{\bar{U}} \right]$$

$$= \rho \bar{U} B^2 \left[C_M u(x,t) + \frac{1}{2} C_M' w(x,t) \right]$$

where C_M is the moment coefficient of the bridge section at the equilibrium position under the steady wind (normally near $\alpha = 0$), and $C_M' = \frac{dC_M}{d\alpha}$ is for the same position; the gust velocity components are $u = u(x,t)$ (horizontal) and $w = w(x,t)$ (vertical) at point x of the span.

Let $S_u(n)$ and $S_w(n)$ be respectively the single-point wind-gust spectra of u and w . These spectra may be assumed uncorrelated, so that their cross-correlations are negligible, i.e. $S_{uw} \approx S_{wu} \approx 0$. The corresponding point-to-point lateral complex cross-spectra, namely $S_u(x_A, x_B, n)$ and $S_w(x_A, x_B, n)$, between spanwise points $x = x_A$ and $x = x_B$, may be

assumed to have negligible imaginary parts (reflecting the near-homogeneity of the atmospheric turbulence) but to exhibit coherence that falls off exponentially according to the factor [5.2].

$$e^{-C|x_A - x_B|/L}$$

where, conservatively (inasmuch as the factor 7 is used):

$$(5.10) \quad C = \frac{7nL}{\bar{U}} \quad .$$

Under the above assumptions and conditions, the cross power spectral density of the applied moment between x_A and x_B is

$$S_{M_\alpha}(x_A, x_B, n) \approx (\rho \bar{U} B^2)^2 x [C_M^2 S_u(n) + \frac{1}{4} C_M'^2 S_w(n)] x e^{-C|x_A - x_B|/L} .$$

Hence, following (5.2) and (5.8), the power spectral density of $\alpha_r(x)$ is given by

$$(5.12) \quad S_{\alpha_r}(x, n) = \alpha_r^2(x) |A_r(n)|^2 \left(\frac{\rho \bar{U} B^2}{I_r}\right)^2 \int_0^L \int_0^L \alpha_r(x_A) \alpha_r(x_B) [C_M^2 S_u(n) + \frac{1}{4} C_M'^2 S_w(n)] e^{-C|x_A - x_B|/L} dx_A dx_B$$

where

$$(5.13) \quad |A_r(n)|^2 = \left\{ \left[1 - \left(\frac{n}{n_r} \right)^2 \right]^2 + \left[2 \gamma_r \frac{n}{n_r} \right]^2 \right\}^{-1} (2\pi n_r)^{-4}$$

The double integral over the span in (5.12) may be approximated [5.18],
by

$$(5.14) \quad L^2 \int_0^L \int_0^L \alpha_r(x_A) \alpha_r(x_B) \left[C_M^2 S_u(n) + \frac{1}{4} C_M^2 S_w(n) \right] e^{-C|x_A-x_B|/L} \frac{dx_A}{L} \frac{dx_B}{L} \\ \approx L^2 G_r \left[\frac{2(C-1)}{C^2} \right] \left[C_M^2 S_u(n) + \frac{1}{4} C_M^2 S_w(n) \right]$$

The mean square deflection $\alpha_r(x)$ about equilibrium is then given by

$$(5.15) \quad \sigma_\alpha^2(x) = \int_0^\infty S_\alpha(x, n) dn$$

This entails the integration of products like $|A(n)|^2 S_u(n)$ and $|A(n)|^2 S_w(n)$. If $S(n)$ is either one of the u or w spectra, the integration yields, to a very good approximation [5.21]:

$$(5.16) \quad \int_0^\infty |A(n)|^2 S(n) dn \approx \frac{S(n_r)}{(2\pi n_r)^4} \int_0^\infty \frac{dn}{\left[1 - \left(\frac{n}{n_r} \right)^2 \right]^2 + \left[2\gamma_r \frac{n}{n_r} \right]^2} \\ + \frac{1}{(2n_r)^4} \int_0^\infty S(n) dn$$

The first of these two parts may be termed the "resonant" contribution, and the second, the "background" contribution. The integral in the first has the value

$$(5.17) \quad \int_0^{\infty} \frac{dn}{\left[1 - \left(\frac{n}{n_r}\right)^2 + \left[2\gamma_r \frac{n}{n_r}\right]^2\right]} = \frac{\pi n_r}{4\gamma_r}$$

Next, to obtain the value of the integral over a particular wind power spectral density, the latter quantity must be explicitly prescribed. The following are accepted forms [5.21], for $S_u(n)$ and $S_w(n)$:

$$(5.18) \quad \frac{n S_u(n)}{u_*^2} = \frac{200 f}{(1 + 50f)^{5/3}}$$

$$(5.19) \quad \frac{n S_w(n)}{u_*^2} = \frac{3.36 f}{(1 + 10f)^{5/3}}$$

where

$$(5.20) \quad f = \frac{nz}{\bar{U}}$$

z being the height of the bridge, and u_* is a friction velocity, the value of which depends on \bar{U} and the type of terrain over which the wind approaches the bridge. In fact, \bar{U} , u_* and z are related [5.21] by

$$(5.21) \quad \bar{U} = 2.5 u_* \ln z/z_0$$

where z_0 is a fetch surface roughness length (see Table 5.1 for values of z_0).

From (5.18) and (5.19), there are obtained the following approximate results for the background contributions:

$$(5.22) \quad \int_0^{\infty} S_u(n) \, dn \approx 6 u_*^2$$

$$(5.23) \quad \int_0^{\infty} S_w(n) \, dn \approx 1.70 u_*^2$$

[Note: A value of $1.75 u_*^2$ was used in calculations made in Section 5.3]

The effective intensity of horizontal turbulence implied by (5.18) is 10.4%; that for vertical turbulence implied by (5.19) is 5.6%.

Table 5.1

SURFACE ROUGHNESS LENGTH

Type of Surface	Range of z_0 (meters)		
Sand	0.0001	to	0.001
Sea Surface	0.000003 (calm)	to	0.004 (gale)
Snow Surface	0.001	to	0.006
Mowed Grass	0.001	to	0.01
Low grass, prairie	0.01	to	0.04
Fallow field	0.02	to	0.03
High grass	0.04	to	0.10
Palmetto	0.10	to	0.30
Pine forest, about 50 ft. tall, medium density	0.90	to	1.00
Suburbs, outskirts	0.20	to	0.40
Suburbs, centers	0.35	to	0.45
Large city centers	0.60	to	0.80

Hence σ_α^2 is approximated, from (5.12) and (5.15), by

$$\sigma_\alpha^2 \approx \frac{\alpha_r^2(x)}{(2\pi n_r)^4} \left[\frac{\rho U B^2 L}{I_r} \right]^2 G_r \left[\frac{2(C-1)}{C^2} \right] F(\gamma_r, C_M, C_M', S_u, S_w)$$

or

$$\sigma_\alpha^2 = \frac{\alpha_r^2(x)}{K_r^4} \left[\frac{\rho B^4 L}{I_r} \right]^2 \frac{G_r}{\bar{U}^2} \left[\frac{2(C-1)}{C^2} \right] F(\gamma_r, C_M, C_M', S_u, S_w)$$

where $K_r = \frac{2\pi n_r B}{\bar{U}}$ and

$$F(\gamma_r, C_M, C_M', S_u, S_w) = C_M^2 \left[\frac{(2\pi n_r) S_u(n_r)}{8 \gamma_r} + 6 u_*^2 \right] + \frac{C_M'^2}{4} \left[\frac{(2\pi n_r) S_w(n_r)}{8 \gamma_r} + 1.70 u_*^2 \right].$$

Most long-span bridges have constant section decks over the span; in this case, $I_r = I G_r L$, and (5.24) may be rewritten as

$$(5.25) \quad \sigma_\alpha^2 = \frac{\alpha_r^2(x)}{K_r^4} \left[\frac{\rho B^4}{I} \right]^2 \frac{1}{G_r} \left[\frac{2(C-1)}{C^2} \right] \frac{F(\gamma_r, C_M, C_M', S_u, S_w)}{\bar{U}^2} .$$

5.2 Discussion of Factors Affecting the Variance in Torsion

1. $\alpha_r^2(x)$. Dimensionless modal form squared. No quantitative effect, except variation along the span. Note that its arbitrary magnitude is cancelled by a corresponding effect in the subsequent factor G_r^{-1} .
2. $K_r^{-4} \propto \left(\frac{\bar{U}}{n_r B}\right)^4$ Fourth power of reduced velocity.
3. $\left[\frac{\rho B^4}{I}\right]^2 \propto \left(\frac{\rho}{\rho_s}\right)^2$, where ρ_s = structural density.
4. G_r^{-1} . See Eq. (5.5). G_r remains approximately constant with increasing sinuosity of the mode.
5. $\frac{2(C-1)}{c^2} \propto \frac{\bar{U}}{n_r L}$. A reduced velocity based on span (rather than width).
6. \bar{U}^{-2} . According to meteorological theory (Eq. (5.21)):

$$\bar{U}^2 \propto u_*^2 \ln^2 z$$

7. γ_r^{-1} . γ_r is the net damping ratio, result of combining mechanical and aerodynamic contributions (see Eq. (5.7)), the latter possibly of negative sign. Thus, $\gamma_r \rightarrow 0$ can signify the danger of flutter instability. According to the shape of the curve for the coefficient A_2^* (Figs. 3.2, 3.3), negative aerodynamic damping contributions that may cause $\gamma_r \rightarrow 0$ are most likely to occur at high values of $\frac{\bar{U}}{n_r B}$, i.e. at high mean wind velocities \bar{U} or at low frequencies n_r , or possibly in bridges with narrow decks (B small).

8. $C_M^2(2\pi n_r)S_u(n_r)$. The first factor C_M^2 is the moment coefficient of the deck section at (or near) zero angle of attack. The second is the "resonant" spectral term:

$$2\pi n_r S_u(n_r) \propto u_*^2 \left(\frac{\bar{U}}{n_r z}\right)^{2/3}$$

9. $\frac{C_M^2}{4} (2\pi n_r)S_w(n_r)$. The first factor $C_M^2/4$ is proportional to the square of the rate of change of the moment coefficient of the deck section with change in twist. The second is, as in 8. above, a "resonant" spectral term:

$$2\pi n_r S_w(n_r) \propto u_*^2 \left(\frac{\bar{U}}{n_r z}\right)^{2/3}$$

10. $6 u_*^2, 1.70 u_*^2$. These are "background" terms in the spectral contributions. These terms, while not completely negligible, contribute much less than do the resonant terms. (See later comments on numerical calculations)

If all of the above observations are combined together, the "background" terms being provisionally ignored, it is observed from (5.25) that

$$(5.26) \quad \sigma_\alpha^2 \propto \left(\frac{\bar{U}}{n_r B}\right)^4 \left(\frac{\rho}{\rho_s}\right)^2 \frac{1}{G_r} \left(\frac{\bar{U}}{n_r L}\right) \frac{1}{\lambda n^2 \frac{z}{z_0}} \frac{1}{\gamma_r} C_{M_0}^2 \left(\frac{\bar{U}}{n_r z}\right)^{2/3}$$

where $C_{M_0}^2$ represents either C_M^2 or $C_M'^2$. Taking the square root, one may compact this further to

$$(5.27) \quad \sigma_\alpha \propto \frac{\bar{U}^{2.833} \rho C_{M_0}}{n_r^{2.833} B^2 L^{1/2} \rho_s G_r^{1/2} \gamma_r^{1/2} (z^{1/3} \ln z)}$$

whence the following facts may be concluded. The standard deviation of bridge torsional buffeting response, σ_α , is proportional to:

1. Mean wind velocity as: $\bar{U}^{2.833}$.
2. Air density ρ .
3. The moment coefficient C_M of the deck section (and/or the slope C_M' thereof).

The standard deviation of torsional buffeting response σ_α is also inversely proportional to:

1. Modal frequency n_r as: $n_r^{2.833}$. The exponent "2.833" combines all the effects of structural parameters, lateral coherence of turbulence, and characteristic turbulence falloff at high frequencies.
2. The square of deck width: B^2 ,
3. The structural density ρ_s .
4. The square root of the span: \sqrt{L} . (Longer spans have less coherent turbulence effects overall.)
5. The shape of the mode, as measured by $G_r^{1/2}$.

6. The square root of the net damping γ_r . By Eqn. (5.7), γ_r represents the difference between structural and aerodynamic damping. Aerodynamic damping generally becomes negative (for those bridges with such an aerodynamic pre-disposition), only for relatively high values of $\bar{U}/n_r B$, i.e. for high mean wind velocities, low natural frequencies, or narrow decks.
7. The height z of the deck above the earth's surface, in the form $z^{1/3} \ln z$. This represents the general falloff of turbulence intensity with altitude.

Most of the above observations are in accord with common intuition: buffeting is more pronounced at higher wind speeds; the shape of the section that cuts down wind-induced twisting moment, or does not increase that moment sharply with twist, is desirable against buffeting; the lower frequencies and modes give the highest buffeting response amplitude; high torsional stiffness is therefore desirable; a wider and heavier deck tends to be more stable; greater length of span reduces the chance of coherent turbulence effects (thus some quite vulnerable long-span bridges are defended against coherent buffeting by their great span); greater bridge height, while exposing the deck to higher mean wind velocities, tends to encounter somewhat lesser turbulence effects.

5.3 Examples in Torsion

A number of examples, based on one hypothetical bridge, will be presented below. Instead of choosing the actual parameters of specific bridges as illustrations of the results of the theory, the following approach will be taken.

A set of 6 torsional modes, sinusoidal in character across the main span, will be considered. Attention will be focused on the main span only. The lowest will be a half sine wave, and each higher mode will be assumed to possess one additional half sine wave. Arbitrary but reasonable frequencies $n = 0.1 \text{ Hz}, 0.2 \text{ Hz}, \dots, 0.6 \text{ Hz}$ will be assigned respectively, to the modes described. The response expected in these modes under naturally gusty winds with mean velocities of 30, 60 and 90 mph* at bridge height will be calculated. The combined aerodynamic and structural damping ratio γ_r in torsion will be calculated from equation (5.7), assuming that the mechanical damping ratio is $\zeta_r = 0.01$; the necessary characteristics of the aerodynamic coefficient A_2^* will be taken approximately as illustrated by Fig. 3.2, Bridge 2, (cf [5.18]).

The deck width will be taken as $B = 100 \text{ ft. (30.5 m)}$ and the bridge height as 200 ft. (61 m) with span $L = 4000 \text{ ft. (1220 m)}$. The friction velocity u_* will be calculated from the formula (5.21):

$$u_* = \frac{\bar{U}}{2.5 \ln \frac{200}{0.0164}} = \bar{U}/23.52$$

for an assumed roughness length $z_0 = 0.0164 \text{ ft. (} 5 \times 10^{-3} \text{ m)}$ corresponding to an open sea wind fetch.

* 1 mph = 0.447 m/sec.

The values of the deck section moment coefficient and its derivative will be taken as $C_M = -1$, $C_M' = 3.67$, respectively. The value of sectional moment of inertia per unit span will be taken as $I = 857,000 \text{ lb. sec}^2$ ($3.9 \times 10^5 \text{ kg. sec}^2$), leading to $(\frac{\rho B^4}{I})^2 = 0.077$. Some auxiliary basic data are given in Tables 5.2 to 5.4, below.

Table 5.5 summarizes the results for the three mean wind velocities calculated, i.e. 30, 60, and 90 mph. The columns given represent σ_α^2 (in rad^2), σ_α (in radians), and edge deflection $50 \sigma_\alpha$ (in feet) at the highest point of the mode (based on a $\frac{1}{2}$ deck-width of 50 ft.) Note that the high point of the mode occurs at different points of the span according to the particular mode shape. For example, it occurs at midspan in the first mode, the two quarter-span points in the second mode, etc.

Based on an assumption that the bridge random response will be normally distributed, maximum expected excursions may be taken as from $3.5 \sigma_\alpha$ to $4.0 \sigma_\alpha$. Results for $3.5 \sigma_\alpha$ are presented in Table 5.6 as edge deflections.

TABLE 5.2

Data for $\bar{U} = 30 \text{ mph} = 44 \text{ ft/sec}^*$; $u_* = 1.275 \text{ mph} = 1.87 \text{ ft/sec} (0.57 \text{ m/sec})$

No. of $\frac{1}{2}$ sine waves	G_r	n_r (Hz)	C	$\bar{U}/n_r B$	A_2^*	γ_r	f	S_u	S_w
1	0.5	0.1	63.64	4.40	-0.04	0.0155	0.4545	16.2	14.5
2	0.5	0.2	127.27	2.20	-0.06	0.0183	0.9090	5.3	5.6
3	0.5	0.3	190.91	1.47	-0.04	0.0155	1.3636	2.7	3.0
4	0.5	0.4	254.54	1.10	-0.03	0.0142	1.8182	1.7	1.9
5	0.5	0.5	318.18	0.88	-0.02	0.0128	2.2727	1.2	1.3
6	0.5	0.6	381.82	0.73	-0.015	0.0121	2.7273	0.9	1.0

* 13.4 m/sec.

TABLE 5.3

Data for $\bar{U} = 60 \text{ mph} = 88 \text{ ft/sec}^*$; $u_* = 2.551 \text{ mph} = 3.741 \text{ ft/sec} (1.4 \text{ m/s})$

Mode	G_r	n_r (Hz)	C	$\bar{U}/n_r B$	A_2^*	γ_r	f	S_u	S_w
1	0.5	0.1	31.82	8.80	0.15	Neg.	0.2273	96.2	57.9
2	0.5	0.2	63.64	4.40	-0.04	0.0155	0.4545	32.5	29.0
3	0.5	0.3	95.45	2.93	-0.07	0.0197	0.6818	16.9	17.0
4	0.5	0.4	127.27	2.20	-0.06	0.0183	0.9090	10.6	11.2
5	0.5	0.5	159.10	1.76	-0.05	0.0169	1.1364	7.4	8.0
6	0.5	0.6	190.90	1.47	-0.04	0.0155	1.3636	5.5	6.0

*26.8 m/s

TABLE 5.4

Data for $\bar{U} = 90 \text{ mph} = 132 \text{ ft/sec}^*$; $u_* = 3.826 \text{ mph} = 5.611 \text{ ft/sec} (1.71 \text{ m/s})$

Mode	G_r	n_r	C	$\bar{U}/n_r B$	A_2^*	γ_r	f	S_u	S_w
1	0.5	0.1	21.21	13.20	0.26	Neg.	0.1515	265.5	112.0
2	0.5	0.2	42.42	6.60	0.08	Neg.	0.3030	92.4	67.7
3	0.5	0.3	63.64	4.40	-0.03	0.0142	0.4545	48.7	43.5
4	0.5	0.4	84.85	3.30	-0.07	0.0197	0.6060	30.7	30.0
5	0.5	0.5	106.06	2.64	-0.07	0.0197	0.7576	21.4	21.4
6	0.5	0.6	127.27	2.20	-0.06	0.0183	0.9090	15.9	16.8

*40.2 m/s

TABLE 5.5
SUMMARY OF RESULTS

Mode	30 mph (13.4 m/sec)			60 mph (26.8 m/s)			90 mph (40.2 m/s)		
	σ_α^2	σ_α	Max. edge defl. (ft) $50 \sigma_\alpha$	σ_α^2	σ_α	$50 \sigma_\alpha$	σ_α	σ_α	$50 \sigma_\alpha$
1	2.20×10^{-4}	0.015	0.741	unstable			unstable		
2	4.64×10^{-4}	0.002	0.108	2.2×10^{-4}	0.0148	0.741	unstable		
3	5.82×10^{-7}	7.63×10^{-4}	0.038	2.1×10^{-6}	0.0046	0.229	2.4×10^{-4}	0.0155	0.775
4	1.29×10^{-7}	3.59×10^{-4}	0.018	4.6×10^{-6}	0.0021	0.107	3.8×10^{-5}	0.0062	0.308
5	4.08×10^{-8}	2.02×10^{-4}	0.010	1.5×10^{-6}	0.0012	0.061	1.2×10^{-5}	0.0034	0.170
6	1.60×10^{-8}	1.27×10^{-4}	0.006	5.7×10^{-7}	0.0008	0.038	4.5×10^{-6}	0.0021	0.106

Summary of Table 5.5 in S.I. Units

Mode	13.4 m/s	26.8 m/s	40.2 m/s
	Max. Edge Defl. (m)	Max. Edge Defl. (m)	Max. Edge Defl. (m)
1	0.226	unstable	unstable
2	0.033	0.226	unstable
3	0.012	0.070	0.236
4	0.005	0.033	0.094
5	0.003	0.019	0.052
6	0.002	0.012	0.032

TABLE 5.6
MAXIMUM EXPECTED EXCURSIONS

Mode	30 mph (13.4 m/s)	60 mph (26.8 m/s)	90 mph (40.2 m/s)
	$3.5 \times 50 \sigma_\alpha$ (ft)	$3.6 \times 50 \sigma_\alpha$ (ft)	$3.5 \times 50 \sigma_\alpha$ (ft)
1	2.59 (0.79m)	unstable	unstable
2	0.378 (0.12m)	2.59 (0.79m)	unstable
3	0.133 (0.04m)	0.802 (0.24m)	2.71 (0.83m)
4	0.063 (0.02m)	0.375 (0.11m)	1.08 (0.33m)
5	0.035 (0.01m)	0.214 (0.07m)	0.595 (0.18m)
6	0.021 (0.006m)	0.133 (0.04m)	0.371 (0.11m)

It will particularly be noted that, for the bridge parameters chosen, the system is unstable at three calculated conditions which affect the first and second modes. This reflects the fact that the critical (zero damping) value has been passed through and that flutter has occurred in the mode in question. It further is to be noted that buffeting response amplitude is particularly sensitive to the values of damping present. The choice of parameters used in the examples presented does not portray a long-span bridge that would in fact have acceptable modern standards of stability, the first mode becoming unstable at a wind velocity of less than 60 mph.

The theory behind the present results differs in two points from that of Ref. [5.18] by Scanlan and Gade. In that reference, it is necessary to interpret the spectra S_u and S_w as being expressed in the units (velocity)²/K where K is reduced frequency $\frac{B\omega}{U}$. In the present work, the units of S_u and S_w are (velocity)²/n where n is frequency in Hz. A second point of difference is that the spectral "background" terms are also included in the present work, whereas they were ignored in Ref. [5.18].

Special comments are in order on the factor F appearing in (5.25):

$$F = C_M^2 \left[\frac{(2\pi n_r) S_u(n_r)}{8 \gamma_r} + 6 u_*^2 \right] + \frac{C_M^2}{4} \left[\frac{(2\pi n_r) S_w(n_r)}{8 \gamma_r} + 1.75 u_*^2 \right]$$

For the second mode of the example calculated for 60 mph (26.8 m/s), the following, in proper order, are the numerical values contributing to this factor:

$$\begin{aligned} 1 \left[\frac{2 (0.2) \times 2.322}{8 \times 0.0155} + 6 \right] u_*^2 &+ 3.367 \left[\frac{2 (0.2) \times 2.072}{8 \times 0.0155} + 1.75 \right] u_*^2 \\ &= 1485.2 \quad \text{with} \quad u_*^2 = 13.995. \end{aligned}$$

From this sample calculation, the relative roles of the background versus the resonant contributions of turbulence are seen to be 20% in the C_M^2 term (effects of horizontal gusts) and 8% in the C_M^1 term (effects of vertical gusts). On the other hand, the total vertical gust (second) term contributes 72.2% of the full gust effect. This is primarily due to the high value of the slope C_M^1 of the moment curve. This emphasizes the point that a moment coefficient trend with low slope is a desirable design attribute.

5.4 Discussion and Conclusions Relative to Torsion

Section V to this point has been concerned with bridge torsional buffeting results only, most particularly in the case where the potential for negative damping due to aerodynamic characteristics is present.

The theory predicts that the buffeting amplitude, based on the important resonance effects and neglecting secondary background turbulence effects, should vary as $\bar{U}^{2.833}$ for any one mode. This fact appears to be reasonably corroborated by Table 5.7 in which theoretically calculated 3.5σ results for Mode 3 (the first that remains stable up to 90 mph (40.2 m/s) are presented for three wind speeds. Assuming that the curve should follow the $\bar{U}^{2.833}$ law exactly at 60 mph (26.8 m/s), results for 30 and 90 mph (13.4 and 40.2 m/s, respectively), can be calculated, based on the empirical formula

$$d = 5.775 \times 10^{-6} \bar{U}^{2.833} \quad *$$

These are also presented in the table, showing reasonable matches.

* Units empirical to convert U (mph) to d (ft). Conversion to S.I. units given in Table 5.7.

TABLE 5.7

MAXIMUM BUFFETING DISPLACEMENTS - TORSION
(Mode 3)

<u>U mph</u>	<u>maximum displacement from example</u>	<u>maximum displacement by curve fit to $\bar{U}^{2.833}$ law</u>
30 (13.4 m/s)	0.133 (0.041 m)	0.113 (0.034 m)
60 (26.8 m/s)	0.802 (0.244 m)	0.802 (0.245 m)
90 (40.2 m/s)	2.71 (0.826 m)	2.53 (0.771 m)

Some experimental encouragement for the theory is obtained by comparing, in the same way, an empirical calculation, based on a $\bar{U}^{2.833}$ law, with experimental buffeting results due to Melbourne [5.13] on a model of the West Gate bridge. These are given in Table 5.8, with the empirical and experimental results assumed to coincide at $\bar{U}_R = 3$. [Law used: $d = 7.92 \times 10^{-4} \bar{U}_R^{2.833}$].

TABLE 5.8

$\bar{U}^{2.833}$ LAW, VERSUS SOME RESULTS OF MELBOURNE

<u>Reduced Velocity \bar{U}_R</u>	<u>Maximum Vertical Displacement d Melbourne</u>	<u>d by $\bar{U}_R^{2.833}$ law</u>
1	0.001 - (0.0003 m)	0.001
2	0.006 - (0.002 m)	0.006
3	0.018 - (0.005 m)	0.018
3.3	0.023 - (0.007 m)	0.023

It should be emphasized that Table 5.7 merely suggests the credibility of the $\bar{U}^{2.833}$ dependence and does not necessarily support other aspects of the theory provided herein.

By empirical curve-fitting to his experimental results, Melbourne [5.13] found that buffeting amplitude was reasonably matched by a law with $\bar{U}^{2.5}$ and $\zeta^{-0.2}$. He did not provide in his empirical expression for the explicit effect of aerodynamic damping as a modifying effect on ζ , but did remark that a $\zeta^{-0.5}$ law (as here) would be expected if no aerodynamic modifying influence were present. The present theory offers an explanation by replacing ζ by γ (cf. eqn. 5.7).

5.5 Theory for Bending

Let $h(x,t)$ be vertical deck deflection at its c.g.. At a spanwise position x , the equation of motion of the section will be

$$(5.28) \quad M[\ddot{h} + 2\zeta_h \omega_h \dot{h} + \omega_h^2 h] = \frac{1}{2} \rho \bar{U}^2 (2B) \\ \times [K H_1^* \frac{\dot{h}}{\bar{U}} + K H_2^* \frac{B\dot{\alpha}}{\bar{U}} + K^2 H_3^* \alpha] + L_h(x,t)$$

where

ζ_h = mechanical damping in bending

ω_h = natural circular frequency in bending

ρ = air density

\bar{U} = mean wind velocity normal to the span

B = deck width

$K = B\omega/\bar{U}$ = "reduced frequency" of vertical motion

H_i^* ($i=1,2,3$) = bridge deck self-excited aerodynamic coefficient

(all H_i^* are functions of $\bar{U}/NB = 2\pi/K$)

h = vertical deflection of c.g. of deck section

$L_h(x,t)$ = aerodynamic buffeting lift per unit span at x .

Let the mode s be a single independent bending mode; then

$$(5.29) \quad h(x,t) = B h_s(x) \xi_s(t)$$

where $\xi_s(t)$ is the associated generalized coordinate. Eq. (5.28) then yields

$$(5.30) \quad M_s [\ddot{\xi}_s(t) + 2\zeta_s \omega_s \dot{\xi}_s(t) + \omega_s^2 \xi_s(t)] = \frac{1}{2} \rho \bar{U}^2 (2B) K H_1^* J_s \frac{LB \dot{\xi}_s(t)}{\bar{U}} + \bar{L}_n$$

where self-excited terms in H_2^* and H_2^* have been dropped on the basis of their relatively small contribution and

$$(5.31) \quad M_s = \int_0^L M h_s^2(x) dx$$

$$(5.32) \quad J_s = \int_0^L h_s^2(x) \frac{dx}{L}$$

$$(5.33) \quad \bar{L}_{h,s}(t) = \int_0^L L_n(x,t) h_s(x) dx$$

Defining a net damping ratio γ_s as

$$(5.34) \quad \gamma_s = \zeta_s - \frac{\rho B^2 L J_s}{2 M_s} H_1^* \left(\frac{\bar{U}}{n_s B} \right)$$

leads to

$$(5.35) \quad B M_s [\ddot{\xi}_s + 2\gamma_s \omega_s \dot{\xi}_s + \omega_s^2 \xi_s] = \int_0^L L_h(x,t) h_s(x) dx = \bar{L}_{h,s}(t)$$

The expression for the aerodynamic buffeting lift force per unit span L_h is given [5.3, 5.18, 5.20] by:

$$(5.36) \quad L_h(x,t) = -\frac{1}{2} \rho \bar{U}^2 B \left[+ 2 C_L \frac{u(x,t)}{\bar{U}} + \left(C_L' + \frac{A}{B} C_D \right) \frac{w(x,t)}{\bar{U}} \right]$$

$$= \rho UB [C_{Lu} u(x,t) + C_{Lw} w(x,t)]$$

where

$$(5.37) \quad C_{Lu} = C_L$$

$$(5.38) \quad C_{Lw} = \frac{1}{2} \left[C_L' + \frac{A}{B} C_D \right]$$

and C_L is the lift coefficient at $\alpha \approx 0$;

C_L' is its slope with respect to angle of attack α ;

C_D is the drag coefficient, lift and drag being based on reference to the deck width B ;

A is the projected frontal area of the deck per unit span.

Using the same type of theory as exposed in relation to torsion, the cross-spectrum of lift between x_A and x_B is found to be

$$(5.39) \quad S_{L_h}(x_A, x_B, n) = (\rho \bar{U} B)^2 [C_{Lu}^2 S_u(n) + C_{Lw}^2 S_w(n)] e^{-C|x_A - x_B|/L}$$

Hence, following (5.29) and (5.35), the contribution of mode s to the power spectral density of $h(x,t)/B$ is given by

$$(5.40) \quad s_{h/B}(x,n) = h_s^2(x) |A_s(n)|^2 \left(\frac{\rho \bar{U} B}{M_s}\right)^2 \int_0^L \int_0^L h_s(x_A) h_s(x_B) [C_{Lu}^2 S_u(n) + C_{Lw}^2 S_w(n)] e^{-C|x_A-x_B|/L} dx_A dx_B$$

where

$$(5.41) \quad |A_s(n)|^2 = \left\{ \left[1 - \left(\frac{n}{n_s}\right)^2 \right]^2 + \left[2 \gamma_s \left(\frac{n}{n_s}\right) \right]^2 \right\}^{-1} (2\pi n_s)^{-4}$$

Using the same integration approximations as noted under the discussion for torsion, and h/B (see eq. (5.29)) for dimensionless vertical displacement, results in:

$$(5.42) \quad \sigma_{h/B}^2(x) \approx \frac{h_s^2(x)}{(2\pi n_s)^4} \left[\frac{\rho \bar{U} L}{M_s}\right]^2 J_s \left[\frac{2(C-1)}{C^2}\right] E(\gamma_s, C_{Lu}, C_{Lw}, S_u, S_w)$$

or

$$(5.43) \quad \sigma_{h/B}^2(x) \approx \frac{h_s^2(x)}{K_s^4} \left[\frac{\rho B^2 L}{M_s}\right]^2 J_s \left[\frac{2(C-1)}{C^2}\right] \frac{1}{\bar{U}^2} E(\gamma_s, C_{Lu}, C_{Lw}, S_u, S_w)$$

where

$$(5.44) \quad E(\gamma_s, C_{Lu}, C_{Lw}, S_u, S_w) = C_{Lu}^2 \left[\frac{(2\pi n_s) S_u(n_s)}{8 \gamma_s} + 6 u_*^2 \right] + C_{Lw}^2 \left[\frac{(2\pi n_s) S_w(n_s)}{8 \gamma_s} + 1.75 u_*^2 \right]$$

Noting that, for typical constant-section decks across the span $M_s = MJ_s L$, (5.43) becomes

$$(5.45) \quad \sigma_{h/B}^2(x) \approx \frac{h_s^2(x)}{K_s^4} \left[\frac{\rho B^2}{M} \right]^2 \frac{1}{J_s} \left[\frac{2(C-1)}{C^2} \right] \frac{1}{\bar{U}^2} E(\gamma_s, C_{Lu}, C_{Lw}, S_u, S_w) .$$

5.6 Discussion of Factors Affecting the Variance in Bending

Clearly, the general arguments about the parameters affecting torsion hold almost in their entirety for the bending case, with the following notes and modifications:

1. $h_s^2(x)$. Same remarks as for $\alpha_r^2(x)$.
2. K_s^{-4} . Same remarks as for K_r , where n_r referred to torsional frequencies; n_s now refers to bending frequencies.
3. $\left[\frac{\rho B^2}{M} \right]^2 \propto \left(\frac{\rho}{\rho_s} \right)^2$
4. J_s^{-1} . Same remarks as for G_r^{-1} .
5. $\frac{2(C-1)}{C^2}$. Same remarks as for torsion, but C is defined for bending modes as $C = 7n_s L / \bar{U}$, so that

$$\frac{2(C-1)}{C^2} \propto \frac{\bar{U}}{n_s L} .$$
6. $\bar{U}^{-2} \propto u_*^2 \ln^2 z$.

7. γ_s^{-1} . This plays a role analogous to γ_r for torsion, but the evolution of typical H_1^* curves vs $\bar{U}/n_s B$ is distinctly different from that of A_2^* curves. H_1^* may reverse sign for some deck geometries as an indication of vortex-related instability. See for example, Fig. 3.2, [5.18] showing H_1^* and A_2^* for a bridge with potential instability at different \bar{U}/nB values in both bending and torsion.

8. and 9. $C_{Lu}(2\pi n_s) S_u(n_s)$; $C_{Lw}(2\pi n_s) S_w(n_s)$

The major elements of difference between bending and torsional aerodynamic contributions lie in the aerodynamic coefficients, C_{Lu} (lift) and C_{Lw} (combination of lift slope and drag effects). It may be concluded that low lift and low lift rate of change with twist, and low drag are all desirable aerodynamic characteristics for a deck section. As before

$$(2\pi n_s) S(n_s) \propto u_*^2 \left(\frac{\bar{U}}{n_s Z} \right)^{2/3}$$

where S is either S_u or S_w .

10. $6 u_*^2$; $1.75 u_*^2$. Background spectral terms. Same comments as earlier.

From the above remarks, it becomes clear that the parameter dependence expressed by relation (5.27) for torsion, holds in the bending

case when the appropriate coefficients are substituted for C_{M0} ; and J_S , γ_S respectively, for G_r , γ_r . Thus, the comments made for Tables 5.7 and 5.8 hold as well for vertical bending deflections. (The deflections cited earlier from Melbourne [5.13] were in fact for vertical bending).

5.7 Examples in Bending

The examples chosen for bending will follow the same general scheme as for torsion. Six sinusoidal modes of increasing sinuosity from 1 to 6 half-sine-waves, and with assumed natural frequencies of 0.1 Hz, 0.2 Hz, ..., 0.6 Hz, will be studied. The main span of a 4000 ft. (1220 m) long bridge will again be the focus. Thus the data items for n_S and J_S , as well as C , f , S_u and S_w , will be the same (cf. Tables 5.2 - 5.4). However, γ_S will depend on the curve used to represent the coefficient H_1^* . For this, see Fig. 3.2. The mass of the deck per unit span will be taken as $M = 711.8 \text{ lb. ft.}^{-2} \text{ sec}^2$ ($3481 \text{ kg sec}^2/\text{m}^2$) and $A/B = 0.13$; $B = 100 \text{ ft.}$ (30.5 m). Also, $C_L = 0$, $C_L' = 2.00$, $C_D = 0.4$.

$$\begin{aligned} \gamma_S &= \zeta_S - \frac{\rho B^2 L J_S}{2 M_S} H_1^* = \zeta_S - \frac{\rho B^2}{2 M} H_1^* = \\ &= 0.01 - 0.0167 H_1^* \\ H_1^* &\approx 0.4 \frac{\bar{U}}{n_S B} \end{aligned}$$

TABLE 5.9

BENDING MODE DATA

Mode	$\bar{U}=30$ mph (13.4 m/s)			$\bar{U}=60$ mph (26.8 m/s)			$\bar{U}=90$ (40.2 m/s)		
	$\frac{\bar{U}}{n_s B}$	H_1^*	γ_s	$\frac{\bar{U}}{n_s B}$	H_1^*	γ_s	$\frac{\bar{U}}{n_s B}$	H_1^*	γ_s
1	4.40	-1.760	0.0394	8.80	-3.520	0.0688	13.20	-5.280	0.0982
2	2.20	-0.880	0.0247	4.40	-1.760	0.0394	6.60	-2.640	0.0541
3	1.47	-0.588	0.0198	2.93	-1.172	0.0296	4.40	-1.760	0.0394
4	1.10	-0.440	0.0174	2.20	-0.880	0.0247	3.30	-1.320	0.0320
5	0.88	-0.352	0.0159	1.76	-0.704	0.0218	2.64	-1.056	0.0276
6	0.73	-0.292	0.0149	1.47	-0.588	0.0198	2.20	-0.880	0.0247

TABLE 5.10

DATA FOR $\bar{U} = 30$ mph* = 44 ft/sec; $u_* = 1.87$ ft/sec

Mode	$\sigma_{h/B}^2$	$\sigma_{h/B}$	$100 \sigma_{h/B}$	max. expected excursion (ft) $3.5 \times 100 \sigma_{h/B}$
1	3.14×10^{-7}	5.60×10^{-4}	0.0560	0.196 (0.060 m)
2	1.18×10^{-8}	1.09×10^{-4}	0.0109	0.038 (0.012 m)
3	1.56×10^{-9}	3.95×10^{-5}	0.0040	0.014 (0.004 m)
4	3.58×10^{-10}	1.89×10^{-5}	0.0019	0.007 (0.002 m)
5	1.11×10^{-10}	1.05×10^{-5}	0.0011	0.004 (0.001 m)
6	4.41×10^{-11}	6.64×10^{-6}	0.0007	0.002 (0.0006 m)

* 13.4 m/s

TABLE 5.11

DATA FOR $\bar{U} = 60 \text{ mph}^* = 88 \text{ ft/sec}$; $u_* = 3.741 \text{ ft/sec}$

Mode	$\sigma_{h/B}^2$	$\sigma_{h/B}$	$100 \sigma_{h/B}$	$3.5 \times 100 \sigma_{h/B}$
1	6.40×10^{-6}	2.53×10^{-3}	0.253	0.885 (0.270 m)
2	3.14×10^{-7}	5.60×10^{-4}	0.056	0.196 (0.060 m)
3	4.74×10^{-8}	2.18×10^{-4}	0.022	0.076 (0.023 m)
4	1.18×10^{-8}	1.09×10^{-4}	0.011	0.038 (0.012 m)
5	3.91×10^{-9}	6.25×10^{-5}	0.006	0.022 (0.007 m)
6	1.56×10^{-9}	3.95×10^{-5}	0.004	0.014 (0.004 m)

*26.8 m/sec

TABLE 5.12

DATA FOR $\bar{U} = 90 \text{ mph}^* = 132 \text{ ft/sec}$; $u_* = 5.611 \text{ ft/sec}$

Mode	$\sigma_{h/B}^2$	$\sigma_{h/B}$	$100 \sigma_{h/B}$	$3.5 \times 100 \sigma_{h/B}$
1	3.39×10^{-5}	5.82×10^{-3}	0.582	2.04
2	1.85×10^{-6}	1.36×10^{-3}	0.136	0.476
3	3.14×10^{-7}	5.61×10^{-4}	0.056	0.196
4	8.30×10^{-8}	2.88×10^{-4}	0.029	0.101
5	2.80×10^{-8}	1.68×10^{-4}	0.017	0.059
6	1.18×10^{-8}	1.09×10^{-4}	0.011	0.038

*40.2 m/sec

REFERENCES FOR SECTION V

- [5.1] Davenport, A.G.: "The Application of Statistical Concepts to the Wind Loading of Structures," Proc. Instn. Civil Engrs., London, U.K., Volume 19, 1961, pp. 449-472.
- [5.2] Davenport, A.G.: "The Response of Slender, Line-Like Structures to a Gusty Wind," Proc. Instn. Civil Engrs., London, U.K., Vol. 23, 1962, pp. 389-407.
- [5.3] Davenport, A.G.: "Buffeting of a Suspension Bridge by Storm Winds," Jnl. Struct. Div., ASCE, June 1962, pp. 233-264.
- [5.4] Davenport, A.G.: "The Action of Wind on Suspension Bridges," Proc. Int'l. Symposium on Suspension Bridges, Lab. Nac. de Engenharia Civil, Lisbon, Portugal, 1966, pp. 79-100.
- [5.5] Davenport, A.G. et al: "A Study of Wind Action on a Suspension Bridge During Erection and on Completion," Rept. BLWT-3-69, Boundary Layer Wind Tunnel Lab., Univ. of Western Ontario, London, Canada, May 1969. Also: Appendix to same, BLWT-4-70, March 1970.
- [5.6] Grillaud, G.: "Les Methodes d'Etude Aerodynamique sur les ponts Suspendus ou à Haubans," Report No. EN ADYM 79-6-R, 1979, Centre Scientifique et Technique du Bâtiment, Nantes, France 1979.
- [5.7] Holmes, J.D.: "Monte Carlo Simulation of the Wind-Induced Response of a Cable-Stayed Bridge," Wind Engrg. Rept. 2/78, Dept. Civ. Engrg., James Cook Univ., No. Queensland, Australia, June 1978.
- [5.8] Irwin, H.P.A.H. and Schuyler, G.D.: "Experiments on a Full Aeroelastic Model of Lions' Gate Bridge in Smooth and Turbulent Flow," Lab. Tech. Rept. LTR-LA-206, National Research Council, Ottawa, Canada, 18 Oct. 1977.
- [5.9] Irwin, H.P.A.H.: "Wind Tunnel and Analytical Investigations of the Response of Lions' Gate Bridge to a Turbulent Wind," Lab. Tech. Rept. LTR-LA-210, National Research Council, Canada, June 1977.
- [5.10] Irwin, H.P.A.H., and Schuyler, G.D.: "Wind Effects on a Full Aeroelastic Bridge Model," Preprint No. 3268, ASCE Spring Convention, Pittsburgh, Pa., April 1978.
- [5.11] Irwin, H.P.A.H.: "Further Investigations of a Full Aeroelastic Model of Lions' Gate Bridge," Lab. Tech. Rept. LTR-LA-221, National Research Council, Ottawa, Canada, May 1978.
- [5.12] Konishi, I., Shiraishi, N., and Matsumoto, M.: "Aerodynamic Response Characteristics of Bridge Structures," Proc. 4th Int'l. Conf. on Wind Effects on Bldgs. and Structures, London, U.K., Sept. 1975, pp. 199-208.

- [5.13] Melbourne, W.H.: "Model and Full Scale Response to Wind Action of the Cable-Stayed Box Girder West Gate Bridge," Proc., Symposium on Practical Experiences with Flow-Induced Vibrations, W. Germany, Sept. 1979 (in press).
- [5.14] Miyata, T., Kubo, Y. and Ito, M.: "Analysis of Aeroelastic Oscillations of Long-Span Structures by Nonlinear Multi-dimensional Procedures," Proc. 4th Int'l. Conf. on Wind Effects on Bldgs. and Structures, London, U.K., Sept. 1975, pp. 215-225.
- [5.15] Miyata, T. and Tanaka, H.: "Aerodynamics of Long-Span Structures," Wind Effects on Structures, Univ. of Tokyo Press, Tokyo, Japan, 1976, pp. 245-256.
- [5.16] Okauchi, et. al: "The Wind-Resistant Experimental Bridge for the Honshu-Shikoku Island Bridge Link" (in Japanese), Res. Rept., Comm. of the Honshu-Shikoku Island Bridge Link Authority, 1976.
- [5.17] Scanlan, R.H.: "Recent Methods in the Application of Test Results to the Wind Design of Long, Suspended-Span Bridges," Rept. No. FHWA-RD-75-115, Federal Highway Admin., Office of R & D, U.S. D.O.T., Washington, DC 1975.
- [5.18] Scanlan, R.H. and Gade, R.H.: "Motion of Suspended Bridge Spans Under Gusty Wind," Jnl. Struct. Div. ASCE, Vol. 103, No. ST9, Sept. 1977, pp. 1867-1883.
- [5.19] Scanlan, R.H.: "The Action of Flexible Bridges under Wind, I: Flutter Theory; II: Buffeting Theory," Jnl. Sound and Vibration, Vol. 60, No. 2, 1978, pp. 187-199 and pp. 201-211.
- [5.20] Shinozuka, M., Imai, H., Enami, Y., and Takemura, K.: "Identification of Aerodynamic Characteristics of a Suspension Bridge Based on Field Data," Stochastic Problems in Dynamics (B.L. Clarkson, Ed.) Pitman, San Francisco and London, 1977, pp. 214-236.
- [5.21] Simiu, E. and Scanlan, R.H.: Wind Effects on Structures, Wiley, New York, 1978.
- [5.22] Wardlaw, R.L.: "Sectional Versus Full Model Wind Tunnel Testing of Bridge Road Decks," DME/NAE Quarterly Bulletin, 1978 (4), pp. 25-47.

VI. CONCLUSIONS

As can be judged from the topics covered: flutter, vortex-shedding, and buffeting, the aim of this report is comprehensive: to include state-of-the-art methods, with examples, that permit the designer to make reasonable estimates of the wind-induced dynamic responses of a long-span bridge.

Sections I and II have offered an introduction with special reference to the pertinent literature of the last decade.

Section III, in reviewing the flutter problem, emphasizes the key parameters that enter into this phenomenon, and points out particularly those that depend upon wind tunnel testing. Also, the two basic kinds of flutter: single-degree torsional ("separated-flow") type and two-degree, coupled ("classical") flutter are identified and described in detail. The examples calculated are for representative bridge parameters. It should be noted that the aerodynamic parameters shown graphically in Figures 3.2 and 3.3, while obtained for very typical bridge deck forms, are not, in the strict sense, extrapolable to new forms of deck section. They are, rather, intended to serve as examples only and do not obviate the need of testing new bridge deck forms to obtain analogous data.

Section IV constitutes a new attempt to fit a simple theoretical model to the observed wind tunnel effects of vortex shedding, and to extrapolate full-bridge behavior from the observed physical action of a bridge-deck section model. The limited aim is to project reasonable estimates of worst-case full-bridge response under coherent vortex shedding. Much remains to be done on the vortex-induced response of bluff bodies in general, under both laminar and turbulent incident flow. Section IV constitutes one small step along this road, which is an open avenue for needed research.

Section V, on bridge buffeting, returns to a topic treated by a number of authors since 1960. In particular, the viewpoint of Gade and Scanlan (1977) is adopted. This point of view incorporates the important information already stored in the bridge flutter derivatives of Figures 3.2 and 3.3. In particular, it includes the case where single-degree torsional flutter instability may be present and may strongly affect buffeting response by bringing damping toward zero. Again, the examples included, worked out for representative bridge parameters, are intended as prototypical calculations that may be followed out in new applications.

The report as a whole is an attempt to present a unified, analytical-experimental aid to engineers concerned with the forecasting of the dynamic responses of long-span bridges to wind. Emphasis is placed upon projections that can be made from section model data only, such models being viewed as both economical and accurate sources of basic aerodynamic data.

